Chapter 1 Cancer Pathobiology

LAK Cytotoxicity against Pancreatic Carcinoma Cells (1)

1. Introduction

Pancreas cancer is one of most aggressively behaving human neoplasms and resectability rates are less than 50%. Lymphokine-activated killer (LAK) cell administration as a therapeutic (2) may be of benefit for patients with pancreatic carcinoma, and especially for those with ascites or multiple liver metastases. This procedure is sometimes associated with vascular leak syndrome characterized by an increase in permeability of many organ vasculatures (3). The syndrome is associated with fluid retention and subsequent functional disorientation in the organs. Activation of the complement system (4) and direct cytotoxicity of LAK cells against vascular endothelial cells (5–7) has been linked to these events. LAK cells induced by IL-2 kill several kinds of non-neoplastic cells *in vitro* (6–8). Cytokines other than IL-2 also induce LAK activity (9–11). Since cytokines have unique physiological functions, different cytokines may induce LAK cells with a different potency or spectrum of specificity. Thus, the presence of cytokines other than IL-2 in the induction phase may modulate LAK cell specificity. We used different cytokines or related substances to modulate LAK activity in an attempt to search for different degrees of lethality for neoplastic and non-neoplastic cells.

2. Establishment of human pancreatic carcinoma cell lines

Eight pancreatic carcinoma cell lines (PCI-6, 10, 19, 24, 35, 43, 55, and 64) of duct cell origin were established from a total of 68 resected or biopsied pancreas cancer tissues. In brief, 1 mm^3 cubes of primary tumor tissue were gently stirred into RPMI-1640 medium supplemented with 1 mg/ml of collagenase type I and 1 TRU/ml of hyaluronidase for 2 h. After washing with RPMI-1640, the dispersed cells were cultured in RPMI-1640 supplemented with 20% fetal bovine serum (FBS). Continuously grown cell lines had a pavement-like arrangement. These cells were passaged by trypsinization and gentle scraping. Their surface adhesion molecule expression has been partly described (12, 13). Established PCI cells ($1x10^7$) were xenotransplanted subcutaneously into BALB/c nu/nu mice. Human umbilical vein endothelial cells (HUVEC) were isolated from human umbilical cords with collagenase and trypsin digestion. HUVEC thus obtained were positively stained for both factor VIII-related antigen and the acetylated low density lipoprotein receptor.

3. Culture in collagen gel matrix

The collagen gel-embedded culture was performed as described but with some modifications (14). The underlying gel (the base layer) was made in a 16 mm plastic dish by pouring 1 ml of the collagen mixture into the plastic dish at 37°C for

10 min. The overlaying gel (the cell layer) was made by the same method as for the base layer, except that the overlaying collagen mixture contained $1x10^5$, enzymatically dispersed PCI cells. The next day, the two-layered gel contained PCI cells was detached from the plastic dish, then was kept floating in a dish with the medium at 37°C with 5% CO_2.

4. Induction of LAK and reagents

LAK cells were induced from peripheral blood lymphocytes (PBL) of healthy volunteers by incubation with cytokines or staphylococcal protein A (SpA) in serum-free media AIM-V (Gibco). In one experiment, LAK was induced in RPMI-1640 or AIM-V media supplemented with or without 10% FBS. The resultant blastic cells were used as LAK cells. Recombinant human cytokines, IL-1β, IL-2, IL-4, IL-6, IL-7, IFN-α, IFN-γ and TNF-α, and SpA were used at each appropriate concentration, as based on the relevant literature (9–11, 15–19).

5. Natural killer susceptibility

Natural killer (NK) susceptibility of each PCI line was examined by the ^{51}Cr release assay. NK-sensitive K562, a human myeloid leukemia cell line, was used as the target positive control.

6. Morphology of the primary, xenotransplanted and collagen gel embedded PCI lines

In the primary sites of our PCI lines (PCI-6, 10, 24, and 43), tumor cells formed a definite, although focally distorted, glandular lumen (moderately differentiated tubular adenocarcinoma), and in the other four (PCI-19, 35, 55 and 64), the neoplastic cells had poorly organized glandular structures (poorly differentiated tubular adenocarcinoma). The histology of each subcutaneously injected, xenotransplanted tumor nodule was adenocarcinoma with focal tubule formation, similar to that from the primary sites. Intracytoplasmic and extracytoplasmic mucin production was a common histologic finding in the eight cell lines. In collagen gel structure, PCI-6, 10, 24, and 43, but not 19 or 35, generated spheroid structures (Fig. 1). Spheroids formed tubular lumens or were composed of compactly aggregated tumor cells, without any lumens. In PCI-19 and 35, no obvious spheroids were formed and PCI cells in the collagen gel were dispersed and of a spindle shape. In the lumen of the spheroids, periodic acid-Schiff positive, mucicarmine-positive mucous substance was sometimes evident.

7. Doubling time, chromosomal abnormality and natural killer susceptibility of PCI cell lines

Doubling time of each PCI cell line differed from line to line, ranging from 33.6 to 52.8h (Table 1). The chromosomal mode ranged from 68 to 84. Many of PCI cell lines had abnormalities at Number 1, 11 and 17 chromosomes. Neither of PCI

cell lines had NK susceptibility; at the E:T ratio of 25, NK cytotoxicity against PCI-6, 10, 19, 24, 35, and 43 varied from 0 ± 8.5 to 2.0 ± 2.9%, whereas NK killed the control K562 myeloid cell line at 57.8 ± 10.4%. LAK cytotoxicity induced with IL-2 in serum-free medium LAK cytotoxicity induced by exposure to 1000 U/ml of IL-2 for 4 days with either serum-free medium AIM-V, 10% FBS-containing AIM-V, or 10% FBS-containing RPMl-l640 was compared. At virtually all E:T ratios examined, the cytotoxicity generated with the serum-free medium against PCI-24 was significantly lower than seen with FBS-containing media (Fig. 2), thereby demonstrating that FBS had an augmenting action on induction of LAK cell cytotoxicity. Since FBS contains distinct growth factor-like substances, or may interact with exogenously added cytokines (20, 21), serum-free medium was used in subsequent experiments.

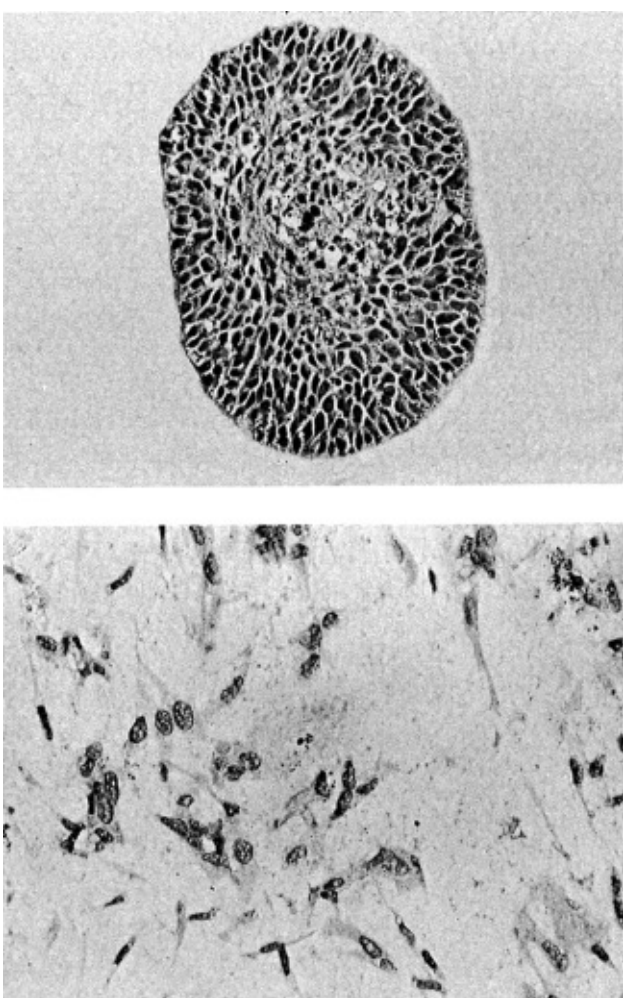

Fig. 1 Histology of PCI cells in collagen gel-embedded culture. PCI-24 shows a spheroid structure (upper). But, the monolayer cell growth is found in PCI-19 culture (lower).

Table 1 Doubling time, cytogenetics, and NK susceptibility of 6 PCI lines.

PCI line	Doubling time (h)	Cytogenetics		NK susceptibility* (% cytotoxicity)
		Chromosome mode	Abnormality	
6	36.0	84	$1q^-$, $3p^-q^+$, $11p^+$ $11q^+$, $17p^+$, $19p^+$	0±8.5
10	34.0	69	$1p^-$, $2p^-$, inv($9p^+q^-$), i(12q), $12p^+$	0±9.6
19	38.4	77	$1q^-$, i(7P), $11p^+$ $11q^+$, $17p^+$, $19p^+$	0.5 ± 0.1
24	39.2	68	$1p^-$, $2q^+$, $3p^+$, $4p^-$, i(7q), $10q^-$	1.9 ± 0.8
35	33.6	76	$1q^-$, i(7p), $11p^+$ $11q^+$, $17p^+$, $19p^+$	2.0 ± 2.1
43	52.8	NT	NT	2.0 ± 2.9

NT: not tested. *: NK susceptibility of K562, as a positive contol of this experiment, was 57.8± 10.4%.

When 1000 U/ml of IL-2 was added to serum-free medium for generating LAK, cytotoxicity against PCI-24 at E:T of 25 with 4 day incubation was maximal, compared with 1, 10, and 14 day incubations. LAK induced with a 14 day treatment showed only a marginal cytotoxicity against PCI-24 cells. Next, LAK was induced with IL-2, at various concentrations, for 4 days. LAK cytotoxicity induced with 1000 U/ml of IL-2 was maximal at E:T ratios of 12, 25, and 50, compared with 1, 10,

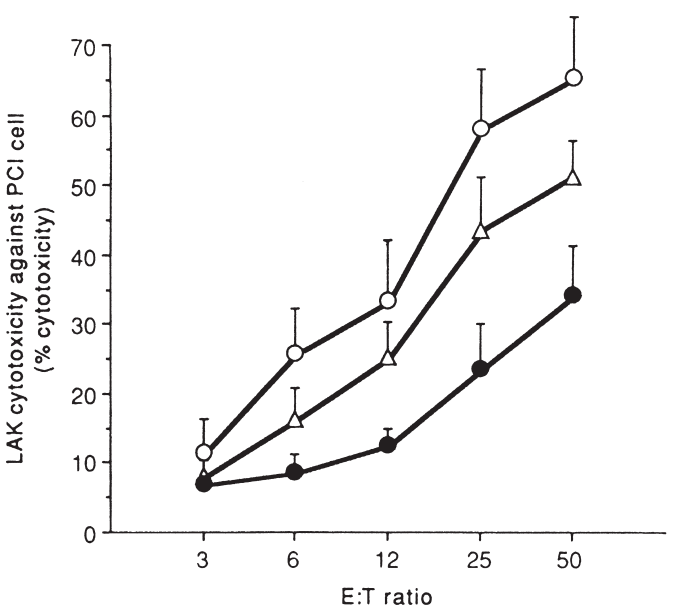

Fig. 2 LAK cytotoxicity against PCI-24. LAK were induced with 1000 U/ml of IL-2. The LAK cytotoxicity were tested under three different conditions, AIM-V medium with 10% FCS (○), RPMI-1640 with 10% FCS (△), or AIM-V medium only (●).

100 and 10,000 U/ml of IL-2. LAK induced with 100 U/ml of IL-2 showed a weak but significant cytotoxicity against PCI-24 at E:T ratios of 25 and 50 in some experiments, but in others, 100 U/ml of IL-2 generated no cytotoxicity. LAK cytotoxicity induced with 10,000 U/ml of IL-2 is slightly lower than that with 1000 U/ml at E:T ratios of 12 or higher, but with no statistical significance.

The IL-2-induced LAK cells also exhibited a potent cytotoxicity against HUVEC, with an increasing cytotoxicity up to 10,000 U/ml of IL-2 added. The intensity of cytotoxicity against HUVEC was equivalent to that seen with PCI cells (Fig. 3). The cytotoxicity against HUVEC by lL-2 (1000 and 10,000 U/ml)-LAK was noted at E:T ratios of 12 or higher. Thus IL-2-LAK, which exhibited a potent cytotoxicity against PCI cells, showed almost equal cytotoxicity against HUVEC.

Our objective, as described next, is to search for LAK-inducing substance(s) against PCI cells as potent as IL-2 (1000 U/ml, 4 days), and to determine if such substances would exhibit a significantly weaker cytotoxicity against HUVEC.

8. LAK cytotoxicity induced with IFN-α, IFN-γ, TNF-α, IL-1β, IL-4, IL-6 and IL-7

A short incubation (up to 24h) of PBL with IFN-α and IFN-γ generated LAK activity (10). When LAK cells induced with 1000U/ml of both IFN for 24h were used in the cytotoxicity assay against PCI-24 cells, these cells exhibited virtually no cytotoxicity. A 48 h incubation of these IFN generated a slight but significant cytotoxicity (Fig. 4), and a 96h incubation exhibited a cytotoxicity similar to that obtained with a 48h treatment. These cytotoxicities were much lower than those

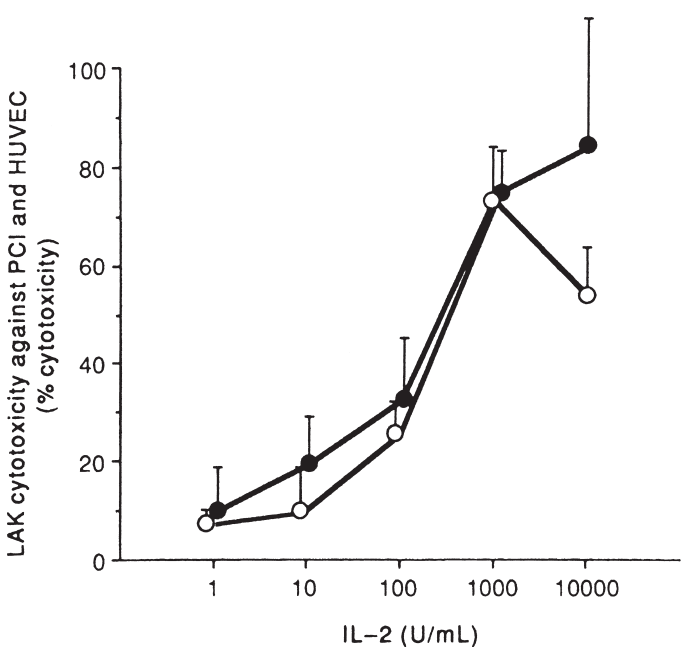

Fig. 3 LAK cytotoxicity against PCI-24 (○) and HUVEC (●). E:T ratio is 50.

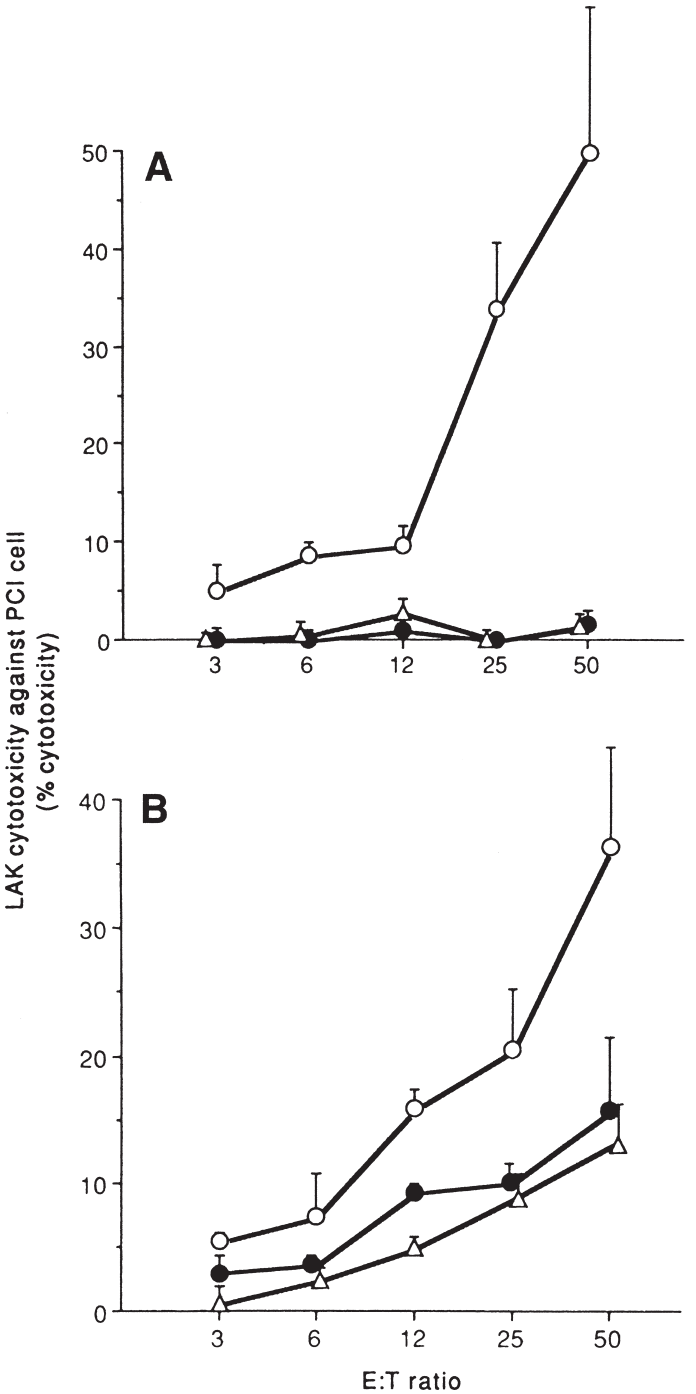

Fig. 4 LAK cytotoxicity against PCI-24. LAK were induced with 1000 U/ml of IL-2 for 4 days (○ in A and B), 1000 U/ml of INF-α for 24 h in A or 48 h in B (△), or 1000 U/ml of INF-γ for 24 h in A or 48 h in B (●).

induced with IL-2 (1000 U/ml) at all E:T ratios examined ($p<0.01$). There was no significant difference between cytotoxicities generated by IFN-α and IFN-γ, except that at the E:T ratio of 12, IFN-γ-LAK showed a significantly higher cytotoxic efficacy than did IFN-α-LAK ($p<0.01$). LAK induced with 1000 U/ml of either IL-6 or IL-7 for 4 days exhibited a cytotoxicity against PCl-24 cells, as was noted with other neoplastic cell lines (Fig. 5) (9, 11). IL-7 generated a significantly greater efficient LAK than IL-6 at E:T ratios of 12 and 25 ($p<0.05$), The cytotoxicity of IL-7-LAK at the E:T ratio of 50 was 36.2%, the most effective cytokine examined other than IL-2 or SpA (see following). However, the cytotoxicity was still much less, compared with that of IL-2 (1000 U/ml). SpA (50 μg/ml, 4 days) induced a potent LAK activity at the E:T ratio of 25. The cytoxicity induced with SpA was even higher than that seen with 1000U/ml of IL-2. When SpA (50 μg/ml) was added to IL-2 (100 U/ml) for 4 days for the induction of LAK, LAK activity was not augmented, compared with LAK induction with SpA alone (Fig. 6). LAK cells induced with 1000 U/ml of IL-4 for 4 days generated no cytotoxic activity at E:T ratios of 3, 6, 12, and 25. At E:T ratios of 50 and 100, a weak cytotoxic activity (% cytotoxicity $<2.5\%$) was evident. IL-1β and TNF-α (both at 1000 U/ml, 4 day) had no LAK-inducing activity against PCI cells at E:T ratios of 3-50.

9. LAK induction with cytokines combined with suboptimal dose of IL-2

As various cytokines have been shown to exert interactions with IL-2 in the induction of LAK activity (9, 15–17, 22), either of IL-1β, IL-6, IL-7, IFN-γ, TNF-α

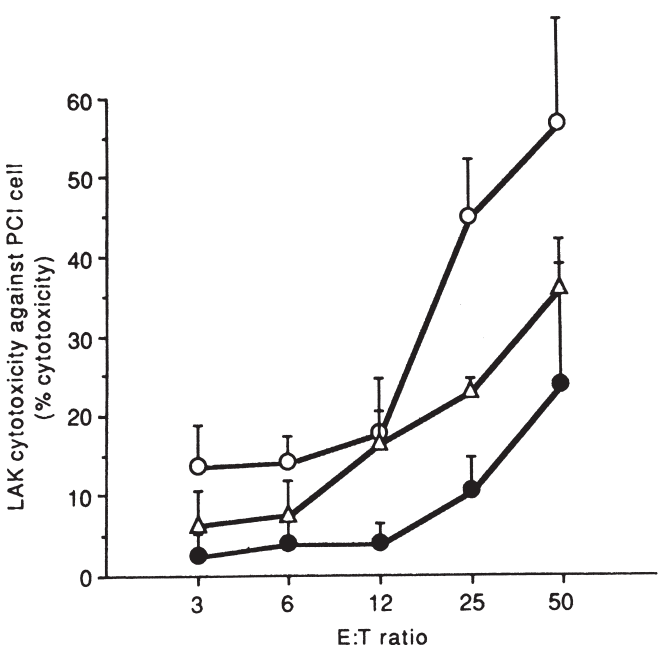

Fig. 5 LAK cytotoxicity against PCI-24. LAK were induced with 1000 U/ml of IL-2 for 4 days (○), 1000 U/ml of IL-7 for 4 days (△), or 1000 U/ml of IL-6 for 4 days (●).

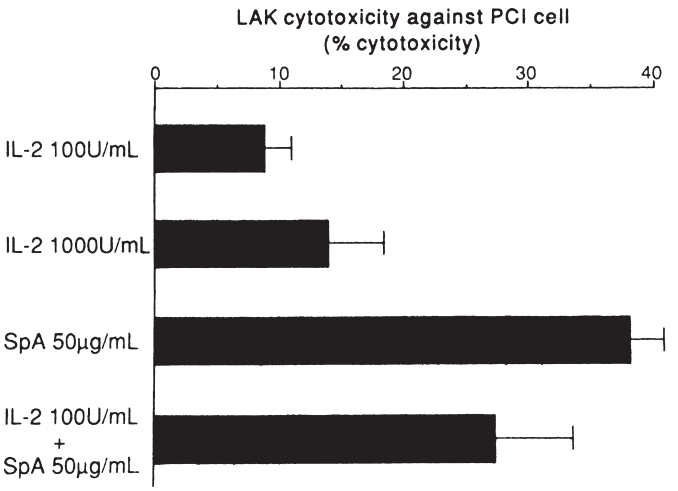

Fig. 6 LAK cytotoxicity against PCI-24. LAK were induced with IL-2 (100 or 1000 U/ml), SpA (50 μg/ml), or IL-2 (100 U/ml) and SpA (50 μg/ml) for 4 days. E:T ratio is 25.

(all at 100 U/ml), or SpA (100 μg/ml) was combined with 100 U/ml of lL-2 in induction, and the LAK cytotoxicity was compared with that seen with a suboptimal dose of lL-2 (100 U/ml)-induced LAK cytotoxicity at the E:T ratios of 3-100. IL-1β, IL-7, or TNF-α, in combination with 100U/ml of IL-2 generated LAK cytotoxicity, but this did not exceed findings with IL-2 (100 U/ml)-LAK. In contrast, the addition of 100 μg/ml of SpA significantly intensified LAK cell cytotoxicity far beyond that which 100 U/ml of IL-2 generated (Fig. 7), although, in this particular experiment, suboptimal IL-2 generated virtually no cytotoxicity. In a separate experiment, IL-6 and IFN-γ exerted no additive effect in inducing LAK cytotoxicity, in combination with 100 U/ml of IL-2.

10. LAK cell cytotoxicity against HUVEC

These experiments revealed that SpA either alone or in combination with 100 U/ml of IL-2 could induce LAK activity against PCI cells, to the extent seen in the case of induction with 1000 U/ml of IL-2. When the cytotoxicity of SpA-induced LAK against HUVEC was compared to that against PCI cells, as shown in Fig, 8, LAK exhibited strong cytotoxicity against HUVEC, under both conditions (1000 U/ml of IL-2, and 100 U/ml of IL-2 combined with 100 μg/ml of SpA). LAK even killed HUVEC more effectively than it did PCI-24 ($p<0.05$).

11. LAK cell population determined by flow cytometry

Surface functional molecules variously induced on LAK cells were analyzed by flow cytometry to search for possible differences in LAK cell constituents (Table 2). As LAK cells are composed mainly of blastic lymphoid cells with T lymphocyte and NK markers (23), LAK cells were exposed to antibodies against T cell (CD3) and

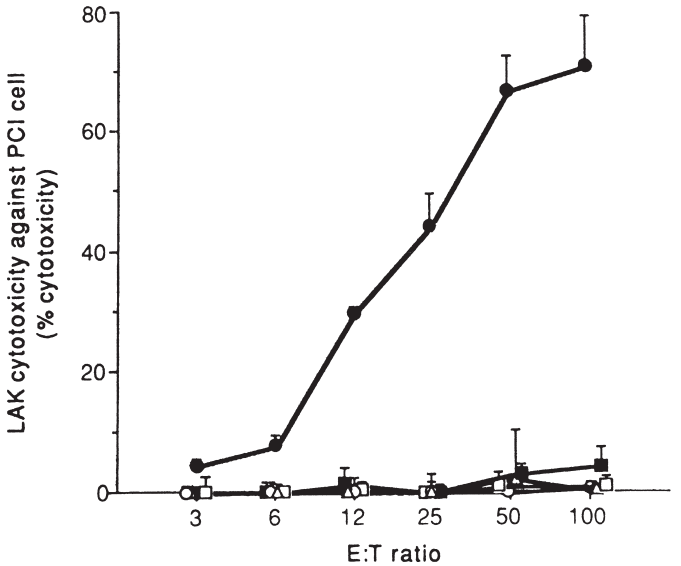

Fig. 7 LAK cytotoxicity against PCI-24. LAK were induced with 100 U/ml of IL-2 (○), IL-2 (100 U/ml) and SpA (100 μg/ml) (●), IL-2 (100 U/ml) and TNF-α (100 U/ml) (△), IL-2 (100 U/ml) and IL-7 (100 U/ml) (□), or IL-2 (100 U/ml) and IL-1β (100 U/ml) (■).

NK cell (CD16 and CD56) markers. In LAK cells induced with IFN for 1 day, cells with NK markers were less numerous than in those induced with IL-2. Similarly, there were fewer NK marker-positive cells among cytokines, either TNF-α, IL-1β, or IL-7, plus suboptimal dose IL-2 combinations, compared with IL-2 LAK. In an independent experiment, SpA-induced LAK contained a few more CD56-positive

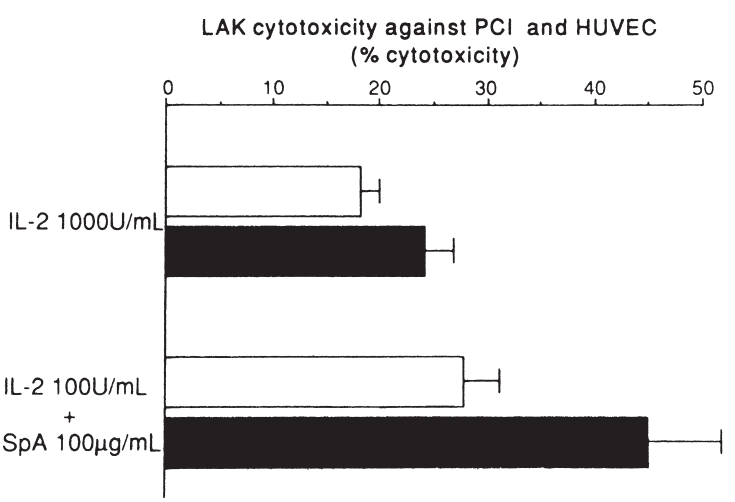

Fig. 8 LAK cytotoxicity against PCI-24 (open bars) and HUVEC (closed bars) at E:T ratio of 25. LAK were induced with IL-2 (1000 U/ml) or IL-2 (100 U/ml) and SpA (100 μg/ml).

Table 2 T and NK marker expression on differently induced LAK cells.

LAK induced with	Induction period (days)	Per cent positivity with T or NK marker CD3	CD16	CD56
Experiment 1				
IL-2 1000 U/mL	4	79.1	42.2	21.5
IFN-α 1000 U/mL	1	51.6	8.2	5.2
IFN-γ 1000 U/mL	1	58.7	15.9	2.7
IL-2 100 U/mL + TNF-α 100 U/mL	4	63.7	14.8	22.7
IL-2 100 U/mL + IL-1β 100 U/mL	4	67.6	7.6	12.6
IL-2 100 U/mL + IL-7 100 U/mL	4	67.3	4.2	13.4
Experiment 2				
IL-2 200 U/mL	4	75.0	11.8	6.2
SpA 100 μg/mL	4	78.2	16.3	14.6

cells than seen with IL-2-induced LAK. There were fewer CDl6-positive blasts in IL-4-induced LAK (1000 U/ml, 4 day), compared with IL-2 LAK.

12. Summary and perspectives

Eight pancreatic carcinoma cell lines of duct cell origin (PCl-6, 10, 19, 24, 35, 43, 55, and 64) were established. Using one of these lines, PCl-24, HUVEC, and several recombinant cytokines, conditions and specificity of anti-PCI LAK induction were investigated, with the focus on a search for LAK activity that differentiates neoplastic (PCI) from non- neoplastic (HUVEC) cells. IFN-γ, IFN-α, IL-4, IL-6, and IL-7, but not TNF-α or IL-1β, induced a weak LAK activity against PCI-24, whereas IL-2-induced (1000 U/ml) LAK exhibited a far more potent cytotoxicity. When these cytokines were added at the suboptimal dose IL-2 (100 U/ml), no significant augmentation in LAK activity was induced. SpA induced LAK activity as potent as that seen with IL-2 (1000 U/ml). Both IL-2-induced and SpA-induced LAK had a potent, dose-dependent cytotoxicity against HUVEC. HUVEC inhibited both IL-2- and SpA-induced LAK cytotoxicity against PCI-24 to almost the same extent as seen with PCI-24. Thus, two potent LAK-inducers did not generate LAK activity that differentiates neoplastic from non-neoplastic cells. Thus, *in vitro* cytotoxicity of LAK against non-neoplastic endothelial cells is unavoidable when handling cytokines in LAK induction.

Cell to Cell Interaction between Carcinoma and Activated Endothelial Cells: Importance of E-Selectin and Sialyl Lewis^a Molecules for Adhesion (13)

1. Introduction

Attachment of carcinoma and endothelial cells is one of the crucial steps in developing blood-borne metastasis, and tumor- cell adhesion to endothelial cells often correlates with metastatic properties *in vivo* (24). At inflamed sites, endothelial cells are activated by inflammatory cytokines, and polymorphonuclear leukocytes or lymphocytes adhere to activated endothelial cells (25, 26), after which transmigration occurs. Similarly, activated endothelial cells also mediate increased attachment to several malignant cell lines, such as melanoma, leukemia, osteosarcoma, and colon carcinoma cell lines (27–30). The cytokine regulation of adhesion between malignant and endothelial cells is thought to be important in the increase in carcinoma metastasis to inflamed sites (31). Pancreas cancers are usually associated with an unfavorable prognosis (32), and blood-borne metastasis to the liver is clearly one of the reasons for this (33). In a colon-cancer cell line, the cells showed an augmented basal adhesion with activated endothelial cells through the Sialyl Lewis^a (SLe^a)/E-selectin interaction (34). Pancreas cancers, most of which are of duct cell origin, frequently produce SLe^a in the form of CA19-9 (35). Therefore, we attempted to clarify whether similar surface molecules are involved in pancreas cancer and activated endothelial cell attachment; 6 of our original pancreas cancer cell lines of duct cell origin were used.

2. Tumor cell/Endothelial cell adhesion assay

The monolayer adhesion assay was performed in a micro-titer plate, as described (36) but with some modification. In brief, HUVEC were cultured in a flat-bottomed, 96-well microtiter plate semi-confluently, and pre-treated with recombinant cytokines. $5x10^4$/well labelled PCI cells were co-cultivated with confluently sheeted HUVEC for 20 min at RT. Following the incubation, the plates were inverted and centrifuged to remove unattached PCI cells. The attached cells were solubilized with 0.1N NaOH, and the radioactivity was measured. The mean $\pm$ standard deviation from quadruplicated wells was calculated. Statistical analysis was performed using Student's *t*-test. Blocking experiments were done using pretreated cells with antibodies, 1H4 (IgG3), 2D3 (IgM), CSLEX1 (IgM), or anti-E-selectin (IgG1). W6/32 (IgG2) was used as a control antibody.

3. Surface adhesion molecule expression on PCI and HUVEC

PCI-6, 10, 19, 24, 35 and 43 cell lines all expressed ICAM-1 and LFA-3. None expressed either VLA-4, a counter receptor for VCAM-1, or LFA-1, Mac-1, or CD43, counter receptors for ICAM-1, as determined by the flow cytometry. SLe^a and SLe^x, counter receptors for E-selectin, were expressed on the cell surface of PCI-10, 24 and 43, but not on that of PCI-6, 19 or 35 (Fig. 9). The SLe^a/SLe^x-positivity of

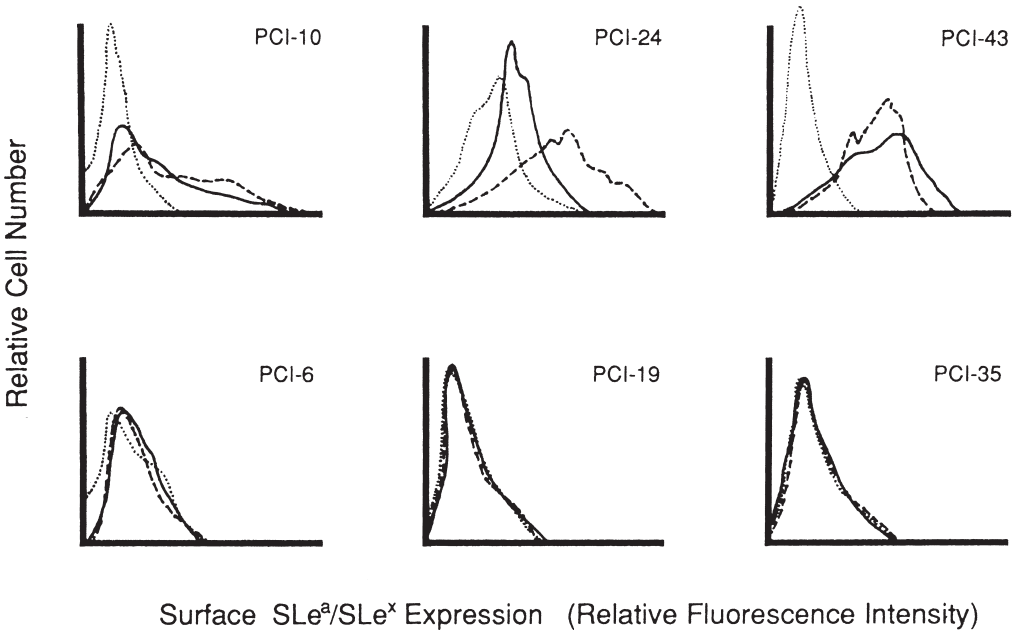

Fig. 9 Surface SLe^a (solid lines) and SLe^x (thick dotted lines) expression on PCI. The backgrounds are shown by thin dotted lines.

PCI cell lines did not correlate with patients' serum CA19-9 levels. Surface SLe^a and SLe^x expression on PCI cells was not regulated by co-cultivation of PCI cells with 100 U/ml of IFN-γ, 25 U/ml of IL-1β, or 100 U/ml of TNF-α for either 4, 24 or 48 h. SLe^x antigen was expressed in PCI-10, 19, 35 and 43, but not in PCI-6 or 24 cells.

HUVEC expressed ICAM-1, and the ICAM-1 expression was increased in the presence of 100 U/ml of IFN-γ, 25 U/ml of IL-1β, or 100 U/ml of TNF-α for 24h. A 4-h treatment of these cytokines did not generate any distinct ICAM-1 induction on HUVEC. Expression of E-selectin and VCAM-1 was negligible on resting HUVEC. VCAM-1 expression was slightly induced by a 4-h treatment of HUVEC with 25 U/ml of IL-1β or 50 U/ml of TNF-α, and the magnitude of VCAM-1 induction was greater after 24 and 48-h treatments than after a 4-h treatment. E-selectin expression was induced by incubating HUVEC with IL-1β or TNF-α, but not IFN-γ for 4 h. Kinetic studies indicated that E-selectin induction by the cytokines reached a peak when HUVEC were treated with cytokines for 4 h, and the induced expression was gradually decreased after 24 h, disappearing almost completely at 48 h. Twenty-five U/ml of IL-1β or 50 U/ml of TNF-α were sufficient to obtain the maximal expression of E-selectin. Five U/ml of IL-1β induced a submaximal expression of E-selectin.

4. Basal adhesion between PCI and HUVEC and regulation by cytokines

Assay revealed a basal adhesion between HUVEC and all the PCI cell lines.

When HUVEC were pre-incubated with 25 U/ml of IL-1β or 100 U/ml of TNF-α for 4 h, PCI-10, 24 and 43 cells showed an increase in attachment, but no such increase was demonstrated in PCI-6, 19 or 35 cells (Fig. 10). Therefore, the augmented attachment of PCI cells to IL-1/TNF-pre-treated HUVEC was closely associated with surface SLe^a/SLe^x expression of PCI cells. IFN-γ (100 U/ml) treatment of HUVEC for 4, 24 and 48 h generated no increase in basal adhesion. The augmented attachment generated by IL-1β pre-incubation between PCI-24 and HUVEC could also be demonstrated by staining the cover slips with Giemsa solution. Increased attachment was evident at both 25°C and 4°C, thus revealing a temperature-independence of this augmentation. Conversely, basal adhesion of PCI cells to non-cytokine-treated HUVEC was reduced at 4°C, as compared with adhesion at 25°C (Fig. 11).

In the following functional experiments, PCI-10 and 24 cell lines were used exclusively, because PCI-43 was established much later than the other PCI lines used. Data obtained from PCI-10 and 24 were essentially identical, and representative data from either PCI-10 or 24 are presented below.

5. Dose effect and kinetics of cytokine regulation of basal adhesion between SLe^a/SLe^x-positive PCI and HUVEC

When HUVEC were co-cultivated with IL-1β at concentrations of 5, 25, 100 and 500 U/ml for 4 h, an increase in attachment, which was not statistically significant, between HUVEC and PCI-24 was observed at 5 U/ml of IL-1β. The augmentation reached a maximum and became statistically significant at IL-1β concentrations of 25 U/ml or higher (Fig. 12). TNF-α at concentrations of 50, 500 and 2,000 U/ml significantly augmented the basal adhesion between PCI-24 and HUVEC. The intensity of augmentation was maximal at TNF concentrations of 50 U/ml or higher. A kinetic study revealed that a 4 h treatment with 25 U/ml of IL-1β was

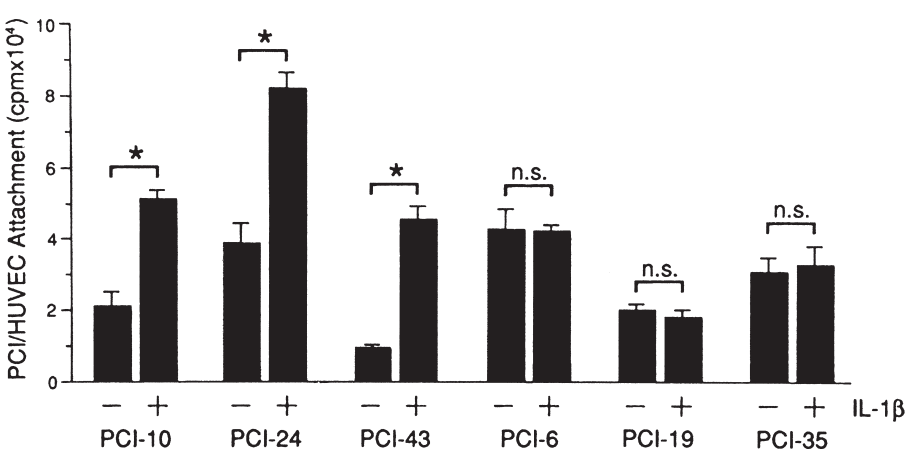

Fig. 10 Basal adhesion between PCI and HUVEC with or without IL-1β (25 U/ml) pretreatments.

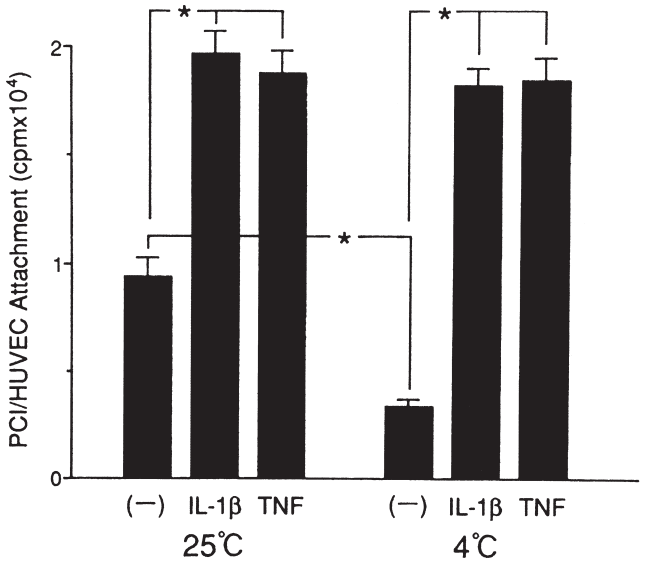

Fig. 11 Effect of IL-1β (25 U/ml) or TNF-α (50U/ml) to basal adhesion between PCI-10 and HUVEC under warm or cold conditions *: $p<0.01$.

effective in augmenting the basal adhesion, whereas a 24 h treatment was less effective (Fig. 12). The dose effect and kinetics data indicate a close association between the augmentative attachment of PCI to HUVEC and surface E-selectin antigen expression on HUVEC.

When 25 U/ml of IL-1β and 50 U/ml of TNF-α were mixed and pre-incubated for 4 h with HUVEC, the extent of the augmented attachment to SLe^a/SLe^x-positive PCI cells was greater than in the case of induction by individual cytokines, and persisted for at least 72 h, although a gradual decrease in adherence was evident during this time (Fig. 13).

6. Blocking of surface adhesion molecules by monoclonal antibodies (MAbs)

Our data indicate that the cytokine-augmented basal adhesion is mediated by the temperature-independent adhesion molecule set; SLe^a/SLe^x on PCI and E-selectin on HUVEC. Addition of anti-E-selectin, but not of the control anti-HLA-ABC MAbs, to the medium of the attachment assay abrogated the augmented basal adhesion of PCI-10 (Fig. 14A) and PCI-24 to almost the level seen in the absence of treatment. Anti-E-selectin treatment had no apparent effect on SLe^a/SLe^x-negative PCI-35 attachment to HUVEC. Anti-SLe^x antibody, in contrast, had no inhibitory effect on the increase in attachment between PCI-10/24 and activated HUVEC. Similarly, the anti-SLe^a antibody 1H4 did not affect the increase in attachment. However, the other anti-SLe^a antibody, 2D3, partially but significantly blocked the increase in attachment between cytokine-activated HUVEC and PCI cells (Fig. 14B).

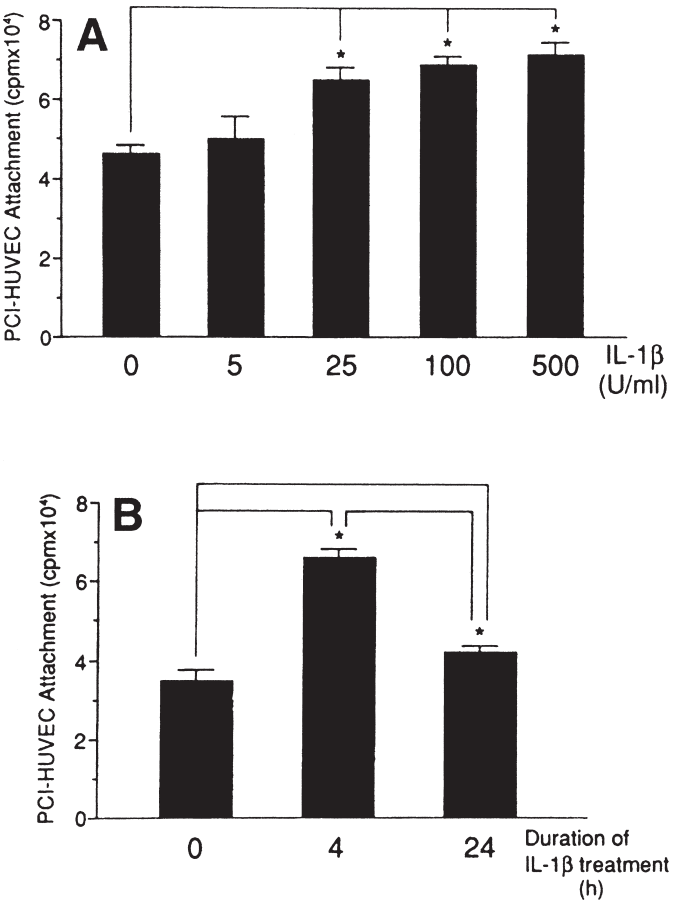

Fig. 12 Dose effect (**A**) and kinetics (**B**) of IL-1β treatment on basal adhesion between PCI-24 and HUVEC. *: $p<0.01$.

7. Summary and perspectives

Adhesion molecules involved in attachment between human pancreatic carcinoma and activated endothelial cells *in vitro* were investigated. Basal adhesion occurred between 6 pancreatic carcinoma cell lines (PCI-6, 10, 19, 24, 35 and 43) and unstimulated HUVEC, and augmented basal adhesion to activated HUVEC was only seen when pancreatic carcinoma cells expressed SLe^a and SLe^x. Activation of HUVEC with IL-1β or TNF-α, but not with IFN-γ, generated the augmentative basal adhesion. Dose dependence and additive effect were observed in augmentation of the basal adhesion induced by IL-1β and/or TNF-α. Increase in adhesion correlated with up-regulation of the surface E-selectin on HUVEC, and was evident at both 25°C and 4°C. Anti-E-selectin and anti-SLe^a blocked the augmented attachment, whereas anti-SLe^x, an antibody against another known ligand for E-selectin, did not. The collective evidence indicates that attachment between pancreatic carcinoma cells and activated endothelial cells is regulated by cytokines such as IL-1β and TNF-α, and is mediated by SLe^a on pancreas carcinoma and E-selectin

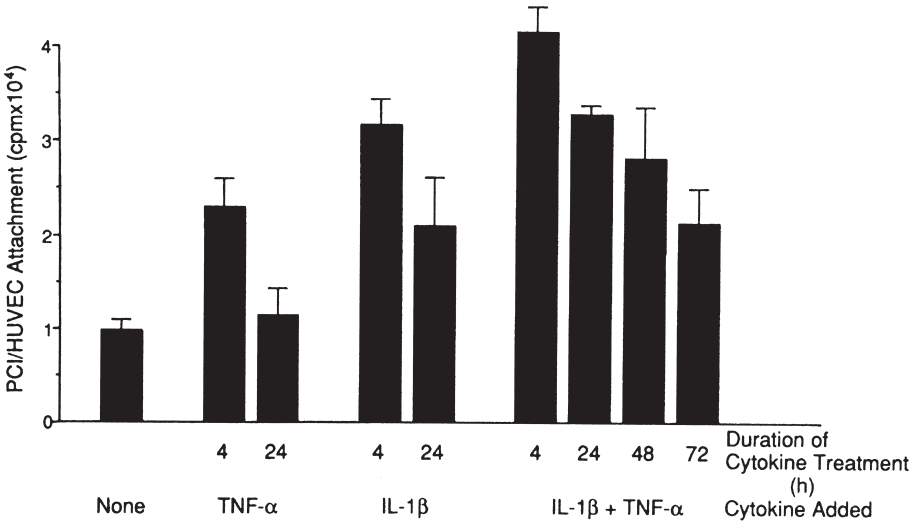

Fig. 13 Mixture effect of IL-1β (25 U/ml) and TNF-α (50 U/ml) on basal adhesion between PCI-24 and HUVEC.

on endothelial cells. These molecules appear to be of significant importance in blood-borne metastasis of pancreatic carcinoma cells to inflamed sites.

Role of SLe^a on Hematogenous Cancer Metastasis (37, 38)

1. Introduction

Metastasis via blood-borne routes, a distinguishing characteristic of malignant neoplasms, follows multistep interactions with host cells. The importance of a property of neoplastic cells with aggressive phenotype has been evaluated in a variety of *in vitro* systems. Attempting to obtain suppression of metastasis *in vivo*, relative contributions among these properties have to be carefully evaluated. To detect one or several major properties essential for blood-borne metastatis *in vivo* may possibly lead to control of metastasis. We searched for correlations between important phenotypes of pancreatic adenocarcinoma cell lines and liver metastasis, using nude and SCID mouse system.

Attachment between carcinoma and endothelial cells is an important process in developing blood-borne metastasis. This attachment *in vitro* was seen to be mediated by E-selectin in several species of carcinoma cell lines (34) (13) and SLe^a on pancreas carcinoma cells is an important ligand for E-selectin on activated endothelial cells (13). These results suggested that these properties exhibited by pancreatic carcinoma cell lines would modulate events related to carcinoma cell-to-endothelial cell attachment, thereby contributing to hematogeneous metastasis in *vivo*. Another objective was to evaluate the *in vivo* importance of these properties on blood-borne metastasis.

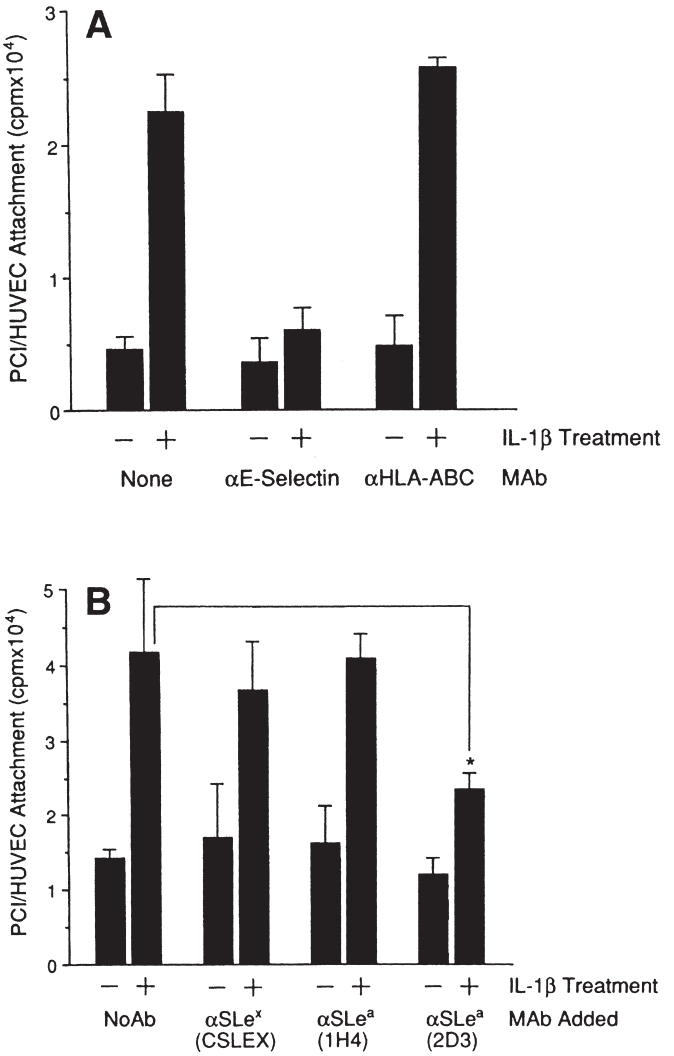

Fig. 14 Effect of MAbs on the augmented basal adhesion. Anti-E-selectin MAb treatment of HUVEC generated complete inhibition of augmented adhesion of PCI-10 (A). 2D3 treatment generated reduced augmentation between PCI-24 and HUVEC (**B**).

2. *In vivo* metastatic system

Male athymic BALB/c nude and SCID (CB-17/Icr-scid Jcl) mice at six-week-old were used. During the experiments, mice were maintained under specific pathogen-free conditions at the Center for Animal Experimentation, Hokkaido University School of Medicine, in accordance with the *Guide for the Care and Use of Laboratory Animals*, Hokkaido University School of Medicine.

Viable PCI cells, $1x10^6$, were inoculated into the exteriorized spleen, using a 27-gauge needle, and the wound was closed with 3-0 prolane. Anti-asialo-GM1 antibody was intravenously administered into the tail vein at -1 day, 1, 2, 3, 5, 7, 14,

21 and 28 days after the PCI injection. Mice were killed 6 weeks later and liver metastasis was evaluated. The entire liver from each mouse was cut evenly into 3 slices and processed for the hematoxylin-eosin (H-E) staining. The number of liver metastatic colonies was microscopically counted as a sum of those from the three H-E slides. For quantitative evaluation of liver metastatic colonies, the number of colonies per unit volume of liver (/cm) was calculated based on the formula reported by Enzmann et al (39). For immunohistochemical staining for SLe^a antigen, 2D3 and NS19-9 were used as the primary antibodies, followed by incubation with biotinylated anti-mouse Ig and avidin-biotin complex

3. Metastatic potential of pancreatic adenocarcinoma cell lines

Nine human pancreatic carcinoma cell lines, PCI-6, 10, 19, 24, 35, 43, 55, 64, and 66, were examined for liver metastatic potential via the portal vein, in anti-asialo-GM1-treated nude mice. In preliminary experiments, the anti-asialo-GM1-treatment in the spleen injection model increased the liver metastasis of PCI-24 cells by about 6 fold at most, as compared with the case of no treatment. In contrast, the intravenous injection of any PCI line, $1x10^6$, from the tail vein rarely generated micrometastases to the lung, even when anti-asialo-GM1 treatment was given.

A variation of metastatic potential was observed among the nine PCI lines, and numbers of liver metastatic colonies in mice given PCI-6, 10, 19, 24, 35, 43, 55, 64, and 66 were 12.7 ± 12.8, 0.3 ± 0.7, 5.0 ± 3.7, 17.0 ± 19.2, 1.2 ± 2.2, 65.9 ± 39.9, 22.0 ± 31.2, 8.3 ± 23.2, and 0.3 ± 0.5, respectively (Fig. 15). A higher metastatic potential was expressed by PCI-43, 55, 24 and 6. PCI-10 and 66 generated minimal liver metastases. Tumor nodules were sometimes generated at sites on the injected spleen, without any cell line-dependent inclination, and formation of these nodules was not related to the development of liver metastases.

4. Correlation of SLe^a positive phenotypes with metastatic property

PCI-10, 24, 43, 55 and 64 (SLe^a-positive lines) but not PCI-6, 19, 35 and 66 (SLe^a-negative lines) expressed SLe^a on their surfaces (Fig. 15). A comparative analysis between SLe^a-positive and -negative lines was made to investigate whether this expression would correlate with the metastatic potential. When all of the SLe^a-positive or -negative PCI lines were grouped and the numbers of metastatic liver colonies from the two groups were collected, the number in SLe^a-positive lines was 21.6 ± 33.9, a figure more numerous than that of SLe^a-negative lines, 6.5 ± 14.3 ($p<0.01$) (Fig. 16). On the other hand, the incidence of liver metastasis, irrespective of the number of colonies of SLe^a-positive (62.5%, or 30/46) and -negative (67.9%, or 22/38) lines, did not differ.

Mean values of surface SLe^a expression from a total of 5,000 cells from PCI-6, 10, 19, 24, 35, 43, 55, 64, and 66 lines were 34.88, 121.87, 20.33, 202.13, 20.95, 381.37, 329.93, 258.82, and 18.7, respectively. There was a statistically significant correlation between surface SLe^a expression intensities and the number of liver metastasis ($p<$

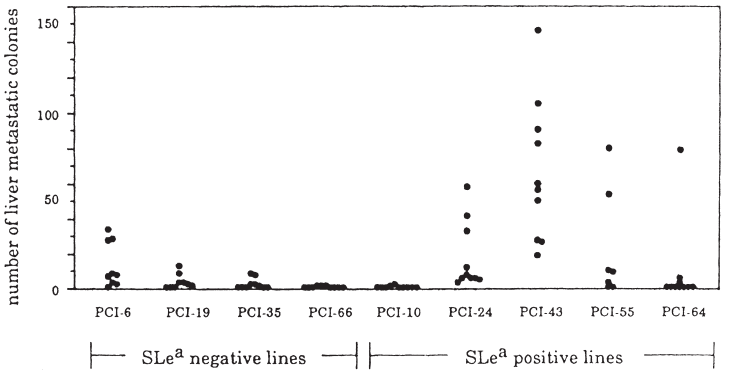

Fig. 15 Potentials of PCI lines for metastasis to the liver. PCI lines were grouped into surface SLe^a-positive and -negative.

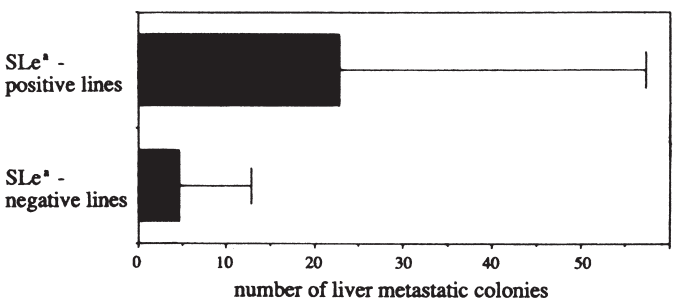

Fig. 16 Frequency of metastatic colonies to the liver in SLe^a-positive and -negative PCI groups.

0.01) (Fig. 17).

5. Effect of anti-SLe^a antibody treatment

To determine if the observed difference in metastatic frequency could be attributed to the surface expression of SLe^a, MAb for SLe^a or for an unrelated PCI antigen was inoculated into the mice. When mice were injected with anti-SLe^a, 2D3 or a control, I-83, the number of liver metastatic colonies of PCI-43-injected mice was dramatically reduced (0.8 ± 1.2 and 6.1 ± 6.5, respectively), when compared with findings when only the vehicle PBS was injected (27.2 ± 30.4) ($p < 0.01$ and $p < 0.05$, respectively). More importantly, 2D3-treated mice had fewer metastatic colonies than did the I-83-treated mice ($p < 0.025$) (Fig. 18). While body weights of mice of 2D3-, I-83-, and PBS-injected groups did not differ, liver weights slightly but significantly differed; the 2D3-injected livers were lighter ($p < 0.05$) (1.56 ± 0.08 for 2D3-, 1.62 ± 0.11 for I-83-, and 1.69 ± 0.08 for PBC-injected group).

The marked inhibitory effect generated by the control I-83 MAb treatment suggested that complement-dependent cellular cytotoxicity (CDCC) may function, and that reactivity to natural antibodies in nude mouse sera against individual PCI cell surface might correlate with the metastatic phenotype. All nine PCI lines

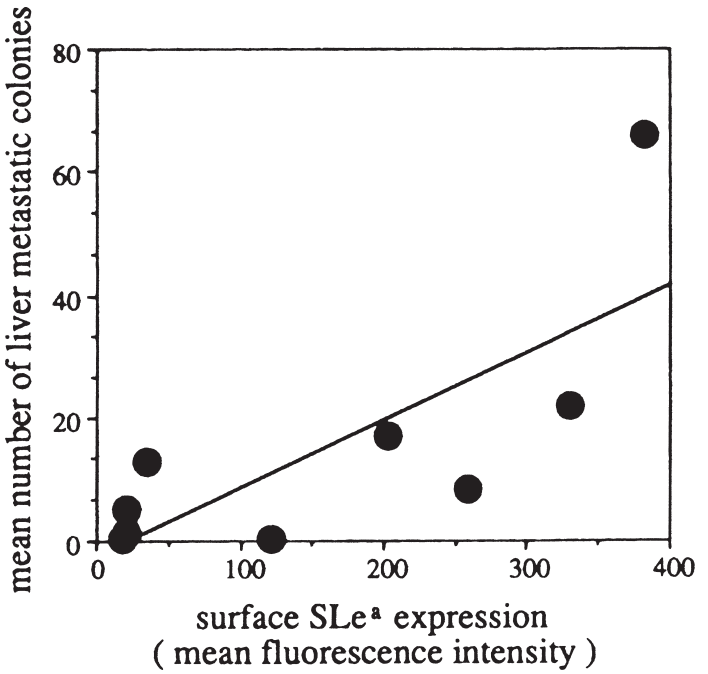

Fig. 17 Correlation between intensities of surface SLe^a expression and the number of colonies of liver metastases in each PCI lines ($p<0.01$).

reacted with undiluted sera from the nude mice. Indirect flow cytometry, using anti-mouse IgG- and IgM-specific immunoglobulin, revealed natural antibodies to be IgM. Reactivity for natural antibodies against each PCI line did not differ from line to line, and there was no apparent correlation between the reactivity and metastatic phenotype. Mean intensities of determinants for natural antibodies on each PCI line were in a range of 10.6 to 21.1, being far less intense than expression of 2D3 and I-83 antigens on PCI-43 cells (in a separate experiment, expression intensities of these antigens on PCI-43 were 333.9 and 445.2, respectively).

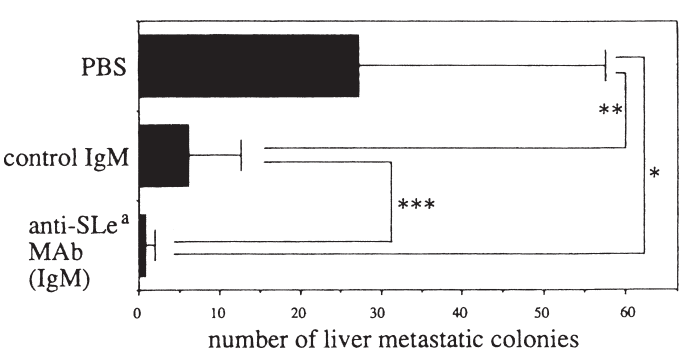

Fig. 18 Inhibitory effect of anti-SLe^a antibody on the number of metastatic colonies in PCI-43-injected nude mice. *: $p<0.01$, **; $p<0.05$, ***, $p<0.025$.

6. Correlation between other PCI phenotypes and liver metastatic potential

Doubling times of PCI-6, 10, 19, 24, 35, 43, 55, and 64 were 5.3, 3.3, 4.4, 2.3, 3.7, 2.7, 2.2, and 5.6 days, respectively. There was no significant correlation between these figures and the numbers of metastases. While all PCI lines produced IL-1α, none produced TNF-α. There was no correlation between the number of metastatic colonies and the amount of IL-1α produced. Gelatinase activities were never evident by zymography, except for evidence of 72 kDa collagenase A in PCI-66 culture supernatants. Thus, there was no correlation between gelatinase activity and metastatic potential *in vivo*. A reverse correlation was observed between ICAM-1 expression on PCI lines and the number of metastatic colonies ($p<0.05$). There was no apparent correlation between other surface antigen expressions, *i.e.*, VLA-4, VLA-6, LFA-1, LFA-3, CEA, E-selectin, VCAM-1, NCAM, Mac-1, HLA-ABC/DR/DQ and ICAM-2, and there was no correlation between the number of metastatic colonies and NK susceptibility, reported by Sugiura *et al*., 1994 (1).

7. Histologic findings of liver metastatic colonies in PCI-43-injected, MAb-treated mice

Metastatic nodules in PBS-injected mice were 3 mm in diameter in the largest ones and microscopic in others. The histologic pattern in this group was poorly differentiated in most areas, but tubular structures with mucin retention were also frequent. Tumor nodules of a larger size had a central fibrosis. Metastatic colonies from 2D3- or I-83-treated mice had a morphology essentially identical with that of the control group, except for the microscopic sizes (Fig. 19). Immunohistochemical staining for SLe^a by 2D3 and NS19-9 revealed a small number of SLe^a-positive PCI cells in metastatic nodules from both 2D3- and I-83-treated mice. Vascular endothelial cells within or adjacent to the metastatic nodules did not stain for SLe^a antigen.

8. Effect of anti-SLe^a and anti-SLe^x treatment on liver metastasis

SLe^a and SLe^x negative PCI-6 cells were injected into the spleen of SCID mice. Compared with PBS-administered group, the number of liver metastatic colonies was reduced in anti-SLe^a (2D3)-administered group ($p=0.012$) (Fig. 20). In anti-SLe^x (CSLEX-1)- and control IgM (I-83)-administered groups, the number of liver metastatic colonies was reduced, but there was no significance compared with PBS group ($p=0.112$ and $p=0.133$, respectively). As regards the average of the largest diameter of colonies in these mice (Fig. 21), a significant reduction was seen in anti-SLe^a (2D3)- and anti-SLe^x (CSLEX-1)-administered groups (both $p<0.03$) compared with the PBS-administered group. On the other hand, there was no significance between PBS- and control IgM (I-83)-administered groups ($p=0.35$). Metastatic colonies in the liver were composed of well to moderately differentiated tubular adenocarcinoma, with some colonies being replaced by microcalcification. There are no obvious differences in tumor morphology in experimetal groups. The

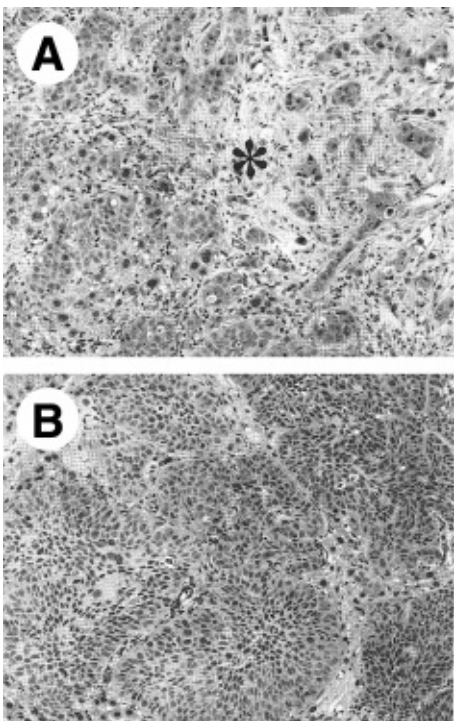

Fig. 19 Histology of liver metastatic colonies. (**A**) A large nodule with central fibrosis (*). (**B**) A smaller nodule with compactly packed carcinoma cells.

density of tumor vessels was not evaluated morphometrically in the present study. The collective evidence indicates that SLe^a/SLe^x antigens have an important *in vivo* role, even in the metastasis of SLe^a/SLe^x-negative tumor cells. This implies

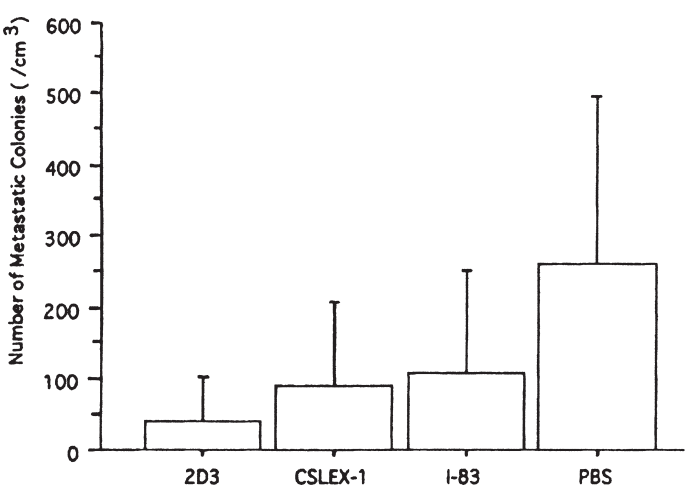

Fig. 20 Inhibitory effect of anti-SLe^a (2D3) and anti-SLe^x (CSLEX-1) antibodies on the number of liver metastatic colonies in PCI-6-injected SCID mice. I-83 and PBS were used as controls for mouse IgM and no antibody added, respectively.

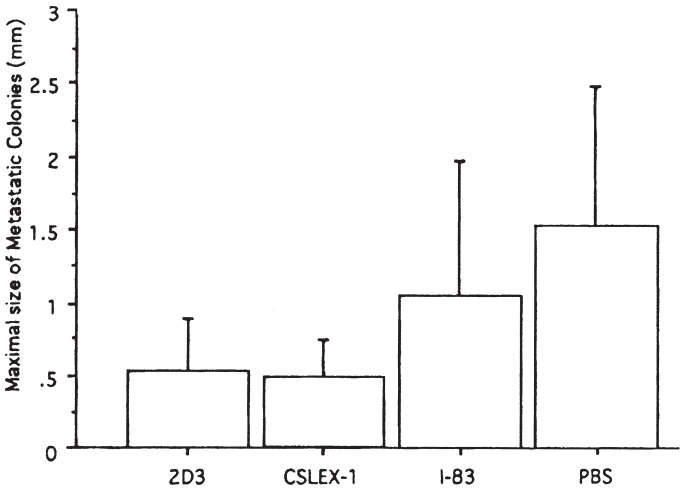

Fig. 21 Inhibitory effect of anti-SLe^a (2D3) and anti-SLe^x (CSLEX-1) antibodies on the largest diameter of liver metastatic colonies in PCI-6-injected SCID mice. I-83 and PBS were used as controls for mouse IgM and no antibody added, respectively.

that there may be an *in vivo* function of SLe^a/SLe^x antigens other than that of the attachment between tumor and endothelial cells.

9. Summary and perspectives

Metastasis to the liver often occurs in patients during the natural course of pancreas cancer. Using 9 established carcinoma cell lines, we examined phenotypes of cell lines to search for correlations with their potential to metastasize to the liver. Anti-asialo-GM1-treated nude and SCID mice were used. PCI-43, -55, -24 and -6, in this order, had frequent metastases, while PCI-10, -19, -35, -64, and -66 did not. *In vitro*-doubling time, surface expression of SLe^a, VLA-4/6, LFA-1/3, CEA, E-selectin, VCAM-1, NCAM, Mac-1, HLA-ABC/DR/DQ, ICAM-1/2, production of IL-1α, TNF-α, and matrix metalloproteinase, and susceptibility to cytotoxicity by natural killer cells were all examined. Expression of surface SLe^a was significantly associated with metastasis; numbers of metastatic colonies of SLe^a-positive and -negative cell lines were 21.6 ± 33.9 and 6.5 ± 14.3 ($p < 0.01$), respectively. Moreover, the intensity of surface SLe^a expression of each PCI line correlated with the number of metastatic colonies in the liver. When anti-SLe^a MAb was administered, the development of liver metastasis by PCI-43 cells was significantly repressed, as compared with a control MAb. Although SLe^a/SLe^x and E-selectin act as a set of adhesion molecules *in vitro*, it is not clear whether the *in vivo* correlation is exclusively mediated by adhesion function. To address this issue, we next investigated whether or not the role of SLe^a/SLe^x antigens on hematogenous metastasis to the liver in SCID mice was exclusively mediated by adhesion, by using antibodies for these antigens and SLe^a/SLe^x-negative, human pancreas adenocarcinoma cell

line PCI-6. The absence of SLe^a/SLe^x expression was supported by the absent flow cytometric detection of the antigens, as well as by the absent attachment augmentation to activated endothelial cells. PCI-6 cells are xenotransplantable to nude and SCID mice, and produce VEGF in a significant amount. PCI-6 cells, $1x10^6$, were injected into spleen of SCID mice, and resultant liver metastases were evaluated six weeks later. An inhibitory effect was observed on the establishment and growth of metastatic colonies when anti-SLe^a or anti-SLe^x antibody was administered. This indicates that SLe^a/SLe^x antigens have an important *in vivo* role even in the metastasis of SLe^a/SLe^x-negative tumor cells. This implies that there may be *in vivo* function of SLe^a/SLe^x antigens other than attachment between tumor and endothelial cells.

Biological Significance of Inflammatory Cytokines Produced by Carcinoma Cells (40–42)

1. Introduction

Several cultured neoplastic cells augmentedly attach to activated endothelial cells (EC) (28–27), observations which may explain the tendency of human malignant tumors to metastasize to inflamed or injured sites. However, the relevance of this observation with respect to metastatic growth of neoplastic cells in apparently non-inflamed, distant organs is unknown. Malignant melanoma cells have been shown to produce IL-1, activating endothelial cells (43), a finding which would explain melanoma cells' adhesion to EC and subsequent metastatic growth at sites without an apparent inflammation. In these *in vitro and in vivo* studies, we show the presence and characteristics of pancreas cancer cell-derived endothelial activating cytokines, IL-1α and IL-6.

2. Enhancement of PCI adhesion to HUVEC by pre-treatment with PCI culture supernatant or co-cultivation with live PCI

Adhesion of SLe^a-positive, SLe^x-positive PCI-24 cells to HUVEC was augmented nearly twofold by incubating HUVEC with 50 U/ml of recombinant human IL-1β for 4 h. Similarly, a preincubation of HUVEC for 4 h with PCI-24 culture supernatants greatly enhanced adhesion of PCI-24 with HUVEC ($p<0.01$). A preceding co-cultivation of 5×10^3/well of "cold", live PCI-24 for 5 h augmented subsequent attachment of $5x10^4$/well of "hot" PCI-24 cells with HUVEC, to the same extent that was obtained by 50 U/ml of recombinant IL-1β or PCI-24 culture supernatant treatment ($p<0.01$, the "cold → hot" experiment) (Fig. 22). Five h pre-incubation of live PCI was necessary for attachment augmentation, the simultaneous presence of 5×10^3 "cold" PCI-24 with 5×10^4 "hot" PCI-24 did not augment the "hot" PCI-24 attachment with HUVEC (the "cold+hot" experiment). Supernatants from other cell lines, PCI-6, 10, 19, 35, and 43 all induced adhesion augmentation between SLe^a/SLe^x-positive PCI-24 and HUVEC, most of which showed a statistical significance

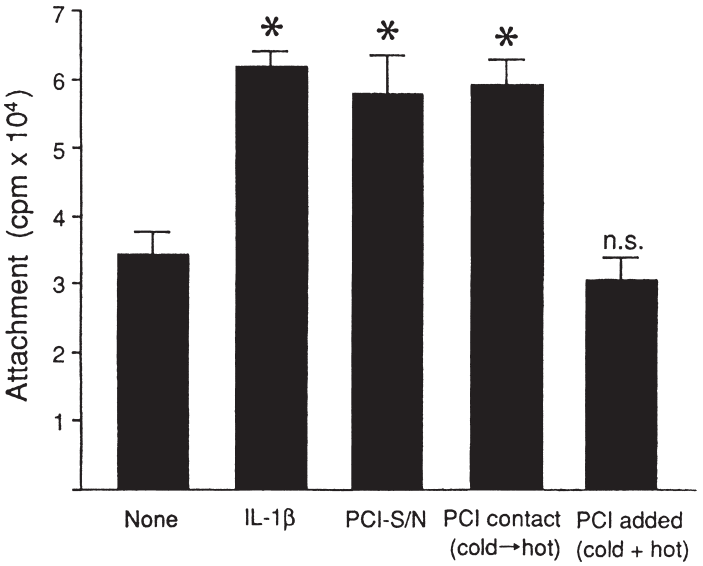

Fig. 22 Attachment between PCI-24 and HUVEC. HUVEC was treated with IL-1β (50 U/ml) or the supernatant of PCI-24 culture (PCI-S/N), or by direct contact with PCI-24 (PCI contact (cold→hot)). As a control, mixed cold and hot PCI-24 were used (PCI added (cold+hot)).

(supernatants from PCI-6, 10, 19 and 35, $p<0.01$, and from PCI-43, not significant).

3. E-selectin induction on HUVEC by pretreatment with PCI culture supernatants or co-cultivation with live PCI

Recombinant human IL-1β at 50 U/ml for 4 h induced E-selectin expression on HUVEC. PCI-24 culture supernatant for 4 h induced E-selectin expression on HUVEC. Co-cultivation of live PCI-24 cells with HUVEC at the ratio of 1:10 for 5 h induced E-selectin expression on the mixture of cells (Fig. 23A). The E-selectin-inducing activity was abolished by the protein kinase inhibitor H7 but not by another protein kinase inhibitor HA1004 or by the calmodulin antagonisit W7 (Fig. 23B). The E-selectin-expressing cells found in the mixed PCI and HUVEC were identified as HUVEC, by light microscopic immunofluorescence staining; the specific staining for E-selectin was mainly found in the cytoplasm of methanol-fixed HUVEC, as coarse granules in IL-1β-treated, PCI-24 culture supernatant-treated, and PCI-24-co-cultured HUVEC. The admixed, spherical PCI cells in the coculture experiment were not stained for E-selectin (Fig. 24). Recombinant IL-2 (2000 U/ml), IL-6 (2000 U/ml), IL-7 (1000 U/ml), IFN-α (2000 U/ml), and IFN-γ (100 U/ml) treatments for 4 h did not induce E-selectin. Culture supernatants from PCI-6, 10, 19, 35, and 43 also induced E-selectin on HUVEC.

Incubation of culture supernatants from PCI-24 for 15, 30 and 60 min did not induce E-selectin. A weak induction was evident when incubation periods exceeded 2 h. E-selectin expression subsided in 12 and 24 h incubations. An extended

incubation of PCI-24 supernatants with HUVEC for 48 h practically abolished the E-selectin-inducible activity. In contrast, the supernatant did not intensify ICAM-1 expression on HUVEC in 4 h, but did augment the expression by 24 and 48 h treatments.

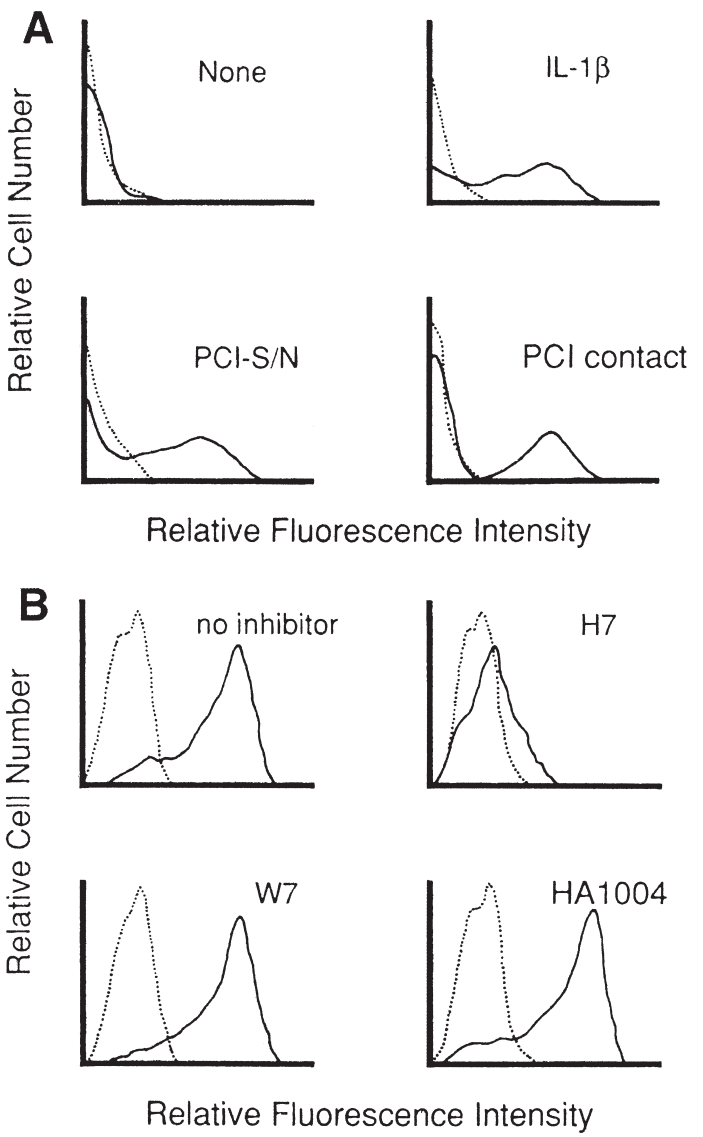

Fig. 23 Induction of surface E-selectin expression on HUVEC by treatment with IL-1β (50 U/ml) or the supernatant of PCI-24 culture (PCI-S/N), or by direct contact with PCI-24 (**A**) and inhibition of the PCI-induced E-selectin expression on HUVEC by H7 (a protein kinase inhibitor), W7 (a calmodulin antagonist) or HA1004 (another protein kinase inhibitor).

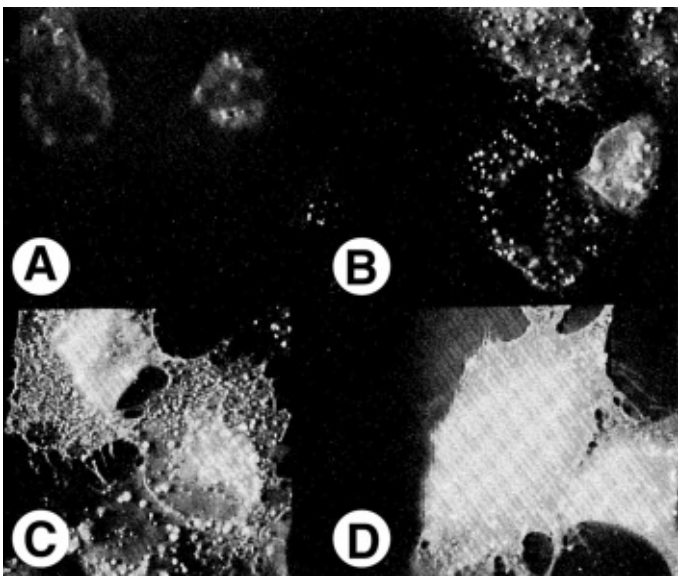

Fig. 24 Immunocytochemistry of E-selectin on HUVEC treated with IL-1β (50 U/ml) (**B**) or the supernatant of PCI culture (**C**), or by direct contact with PCI (**D**). Untreated HUVEC was in **A**.

4. PCI supernatant or pre-incubation with PCI induce increase in PCI-EC adhesion mediated by E-selectin and SLe^a

Anti-E-selectin but not anti-ICAM-1, each at 50 μg/ml concentration, abolished increased adhesion of PCI to EC induced by IL-1β, PCI contact ("cold → hot") and PCI-supernatant (PCI-S/N) (Fig. 25A), revealing that all of the three kinds of enhanced adhesion were E-selectin-dependent. In contrast, the enhanced adhesion was ICAM-1-independent; the anti-ICAM-1 HA58 has been shown to block LFA-1/ICAM-1 interaction in the PCI-to-LAK cell interaction (12). Similarly, anti-SLe^a but not SLe^x antibody treatment inhibited the PCI-supernatant (PCI-S/N)-induced increase in adhesion. Apparently, this augmentation was SLe^a- but not SLe^x-dependent (Fig. 25B), although the observed blocking effect of anti-SLe^a was not so effective as the effect of anti-E-selectin.

5. Cytokine production by PCI cell lines

TNF-α and IL-1α/β in culture supernatants from PCI-24 cells were measured by ELISA. TNF-α was absent in the culture supernatants. A negligible amount of IL-1β was detected ($<$1 U/ml). No detectable E-selectin expression was induced by 1 U/ml of recombinant IL-1β. Instead, 27 to 368 pg/ml of IL-1α was detected in PCI-24 supernatants by the ELISA. Similarly, 39 to 510 pg/ml of IL-1α was detected in other PCI cell line-derived culture supernatants. The northern hybridization analysis revealed IL-1α but not IL-1β or TNF-α mRNA expression in all PCI cell lines tested.

To investigate regulatory functions of exogenous cytokines and growth factors

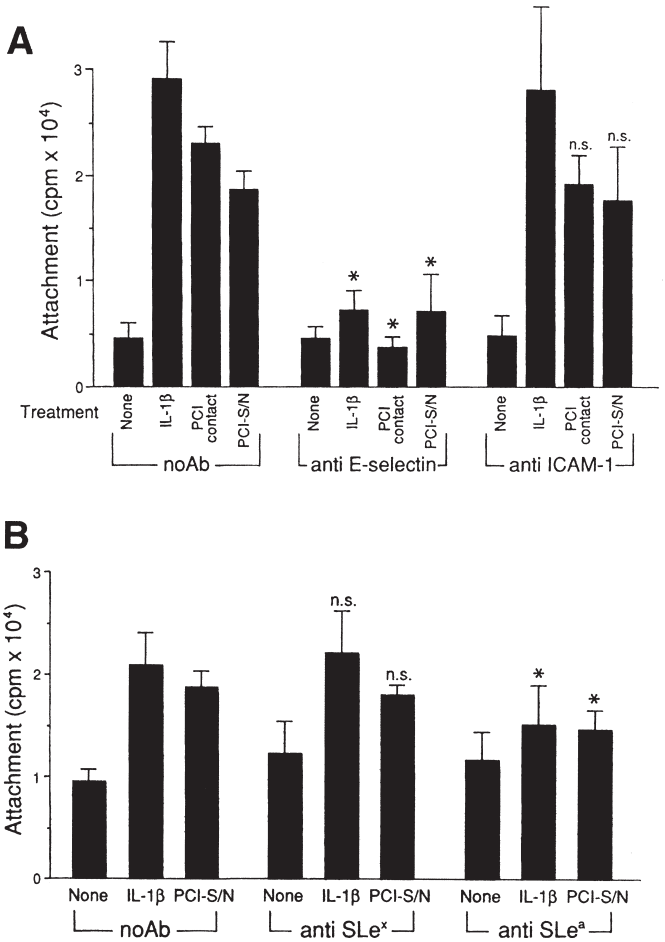

Fig. 25 Blocking of augmented attachment between PCI and HUVEC treated with IL-1β (50 U/ml) or the supernatant of PCI culture, or by direct contact with PCI, by anti-E-selectin or anti-ICAM-1 antibodies (**A**) or anti-SLe^a or anti-SLe^x antibodies (**B**).

on IL-1α production by PCI cells, IL-1α in spent media from PCI-24 cultured with cytokines and growth factors was measured by ELISA. Recombinant human IL-2 (2500 U/ml), IL-1β (1000 U/ml), IL-6 (500 U/ml), transferrin (100 pg/ml) and TGF-β (100 pg/ml) treated for 4 days did not modulate IL-1α release into the culture supernatants. TNF-α (500 U/ml), in contrast, induced a marked increase in IL-1α concentration in the supernatant (Fig. 26). IL-4 (1000 U/ml) and IFN-γ generated a marginal increase in IL-1α in the supernatant ($p<0.01$).

6. Blocking of IL-1 activity in PCI supernatant

Anti-IL-1α antibody at 25 μg/ml almost completely blocked E-selectin-inducing activity of 50 U/ml of recombinant IL-1α, whereas normal rabbit serum did not. The same amount of the anti-IL-1α antibody inhibited most, if not all, E-selectin-

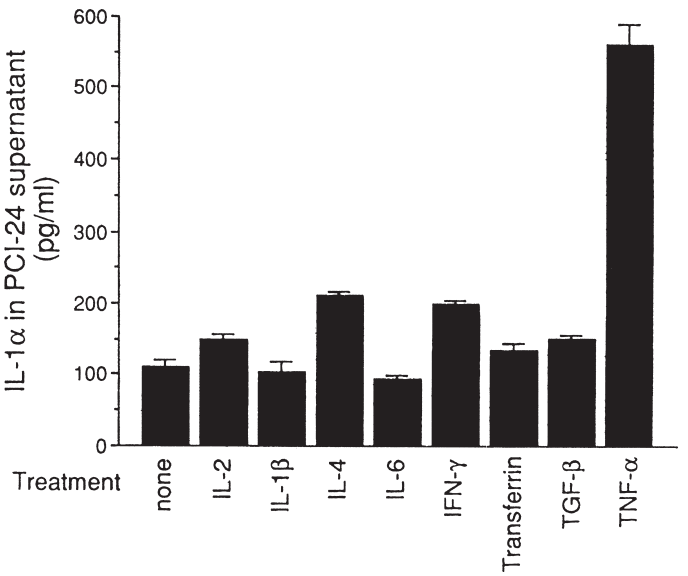

Fig. 26 Modulation of IL-1α production in PCI-24 culture by cytokines.

inducing activity in PCI supernatant (Fig. 27), though normal rabbit serum did not. In contrast, anti-TNF-α and anti-IL-1β antibodies, (which had absorbed activities exerted by recombinant TNF-α and IL-1β, respectively) did not block E-selectin-

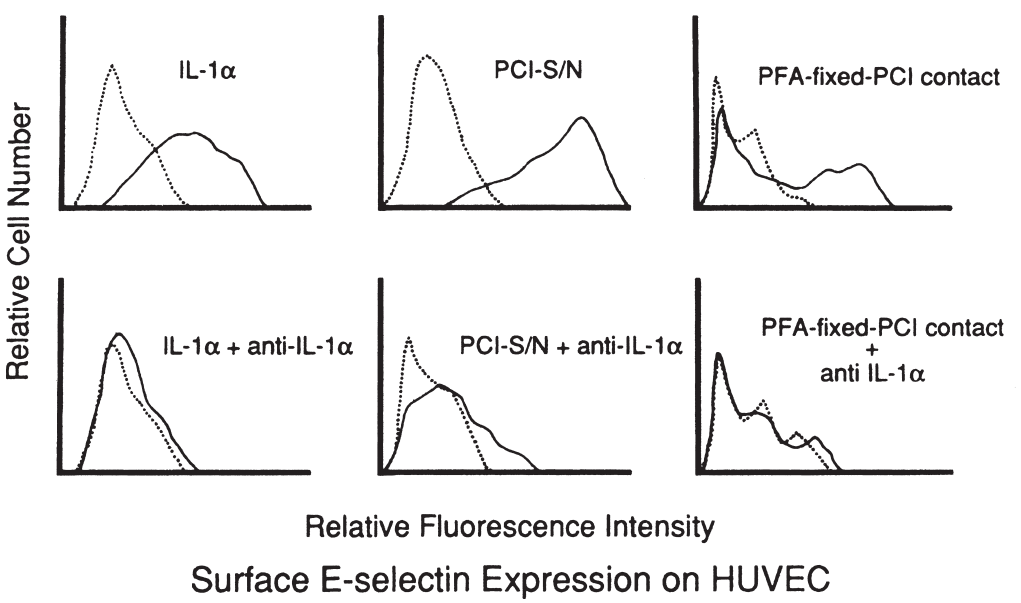

Fig. 27 Absorption of the E-selectin-inducing activity in PCI culture supernatants by anti-IL-1α antibody. Expression of E-selectin on HUVEC treated with the supernatant of PCI-24 culture (PCI-S/N)+anti-IL-1α antibody, or by direct contact with PFA-fixed PCI (PFA-fixed-PCI contact) +anti-IL-1α antibody were compared to HUVEV treated with PCI-S/N or PFA-fixed-PCI contact, respectively, by FACS. HUVEC treated with IL-1α+anti-IL-1α is a control.

inducing activity of PCI supernatants.

7. E-selectin induction on HUVEC by a direct contact with paraformaldehyde-fixed PCI

After 4% paraformaldehyde (PFA)-fixation and subsequent washing, PCI-24 appeared dead and no detectable E-selectin-inducing activity was found in culture supernatants. The PFA-fixed PCI at $5x10^3$/well were incubated with $5x10^4$/well of HUVEC for 5 h, and E-selectin expression on HUVEC was determined by indirect flow cytometry. E-selectin was induced on HUVEC by adding PFA-fixed PCI cells (Fig. 27). The activity exerted by 5×10^3/well of viable PCI cells was more intense than that of PFA-fixed PCI. When PCI cells were treated with anti-IL-1α antibody, and then fixed, the E-selectin-inducing activity was almost completely abolished, indicating the presence of functional, membrane-bound IL-1α on the surface of PCI cells.

8. *In vitro* vascular permeability assay and modulation of *in vitro* permeability by PCI culture supernatants

In vitro permeability assay was done according to Maruo *et al* (44), but with modifications. Briefly, HUVEC were confluently grown on Cell Culture Insert with 0.45 μm multiple pores placed on a 24-well plate. Three hundred μl of the medium containing 2.5 mg/ml Evans Blue bound bovine serum albumin (EBA) were put into the luminal chamber and the preparation then incubated at 37°C. The amount of EBA that passed across the HUVEC monolayer into the abluminal chamber during a 12 h-assay was determined using a spectrophotometer, by measuring OD 620 nm. The data are expressed as permeability index (P.I.).

Addition of supernatants from PCI-10 but not PCI-24 cultures resulted in a significant enhancement of EBA permeability ($p<0.05$) (Fig. 28). Another experiment demonstrated that PCI-6 but not PCI-43 induced an augmented permeability across the monolayers ($p<0.05$). In these experiments, recombinant IL-6 and IL-1α. served as positive controls; these cytokines were shown to be vascular permeability modulators (45–44). Recombinant IL-6 at 500 U/ml mediated a significant permeability increase, ranging from 10 to 40 P.I., presumably depending on the conditions of the umbilical cords. In contrast, recombinant human IL-1α mediated a marginal, non-significant permeability increase, and repeated experiments did not reproducibly lead to permeability augmentations. The protein kinase inhibitors, H7 and HA1004, and the calmodulin antagonist, W7, all at 30 μM, were added in the *in vitro* permeability assay, simultaneously with PCI-10 supernatants. W7 most effectively inhibited the permeability increase generated by PCI-10 supernatants ($p<0.05$), whereas H7 and HA1004 exhibited a non-significant, marginal inhibition (Fig. 29).

9. IL-6 mRNA and protein production by PCI cell lines

As recombinant IL-6 induces a permeability increase in experimental animal models (44), we examined IL-6 production by PCI cells. Northern hybridization of IL-6 cDNA with six PCI culture cell lines revealed that PCI-6, -10, -19, and -35, but not -24 or -43 expressed the specific, 1.3 kb mRNA band. ELISA assay demonstrated a production and release of immunoreactive IL-6 protein into culture supernatants by PCI-6, -10, -19, and -35 cells at over 1,200 pg/ml concentrations, while IL-6 production by PCI-24 and -43 was negligible (4.2 and 3.0 pg/ml, respectively).

Recombinant IL-6 augmented vascular permeability *in vitro*, in a dose-dependent manner, mediating significant P.I. values at concentrations of 500 U/ml or higher (Fig. 30). To determine if an intracellular signal transduction pathway mediates the permeability modulation by IL-6, H7, HA1004, and W7 were included in the assay system. All these signal transduction blockers significantly inhibited the permeability generated by 500 U/ml of IL-6 (H7, $p<0.05$; W7, HA1004, W7+H7, and W7+HA1004, $p<0.01$) (Fig. 31).

10. Absorption of modulator activity of PCI supernatants by anti-IL-6 antibody

We first examined the validity of use of anti-IL-6 antibodies in the *in vitro* monolayer system in order to consider them for a subsequent absorption experiment. Anti-IL-6 or control mouse IgG was incubated overnight at 4°C with RPMI-1640 medium containing 500 U/ml of recombinant IL-6. Preincubation with anti-

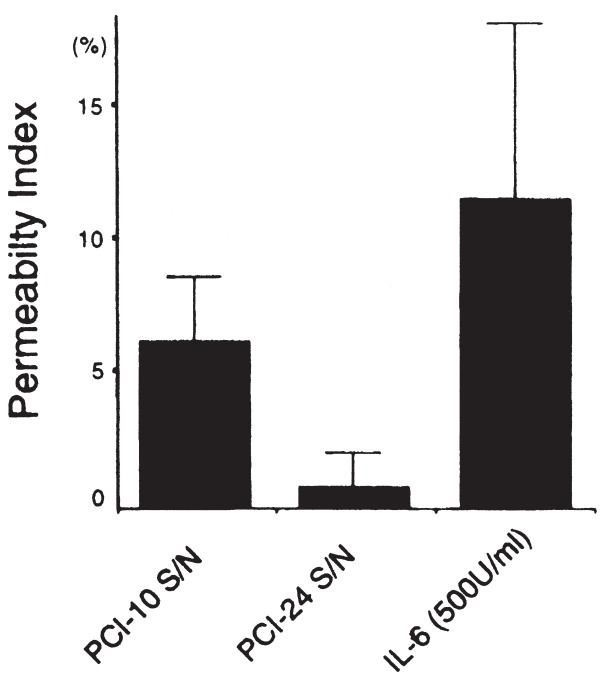

Fig. 28 Modulation of albumin permeability across HUVEC monolayer by PCI culture supernatant (PCI-S/N). IL-6 was used as a control.

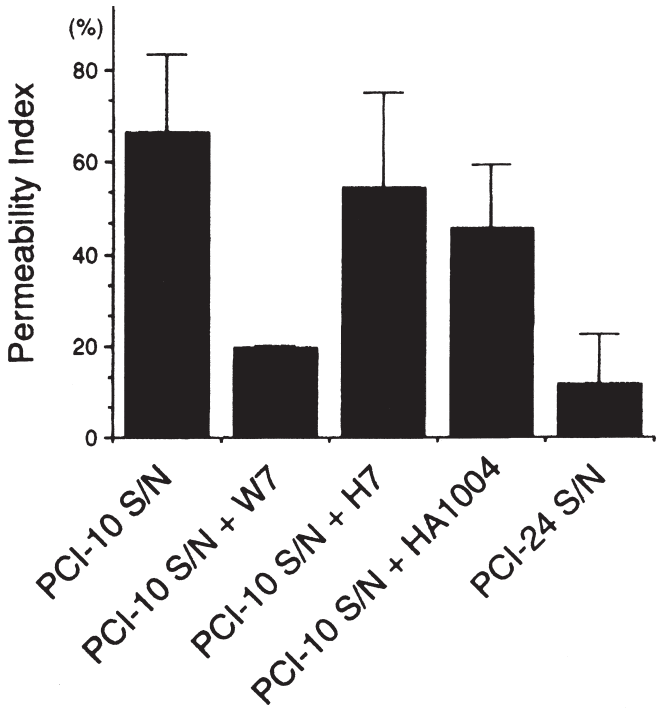

Fig. 29 Effect of protein kinase inhibitors, H7 and HA1004, and a calmodulin antagonist, W7, on albumin permeability across HUVEC monolayer by PCI culture supernatant.

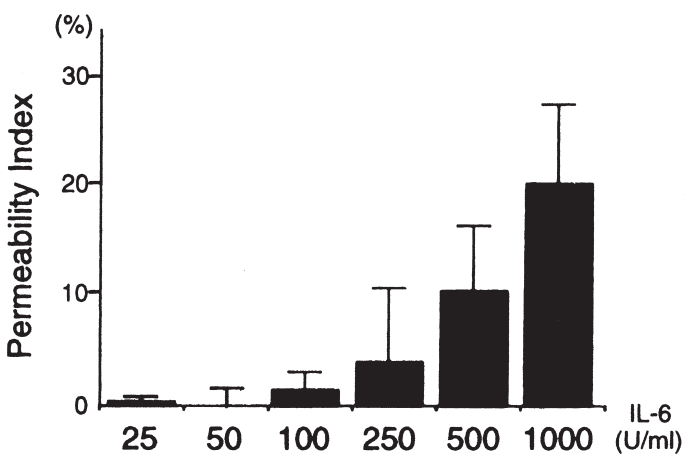

Fig. 30 Dose-dependent action of IL-6 on albumin permeability across HUVEC monolayer.

IL-6 but not control mouse IgG almost completely blocked the enhanced albumin permeability ($p<0.01$) (Fig. 32). Anti-IL-6 or control mouse IgG alone did not modulate permeability.

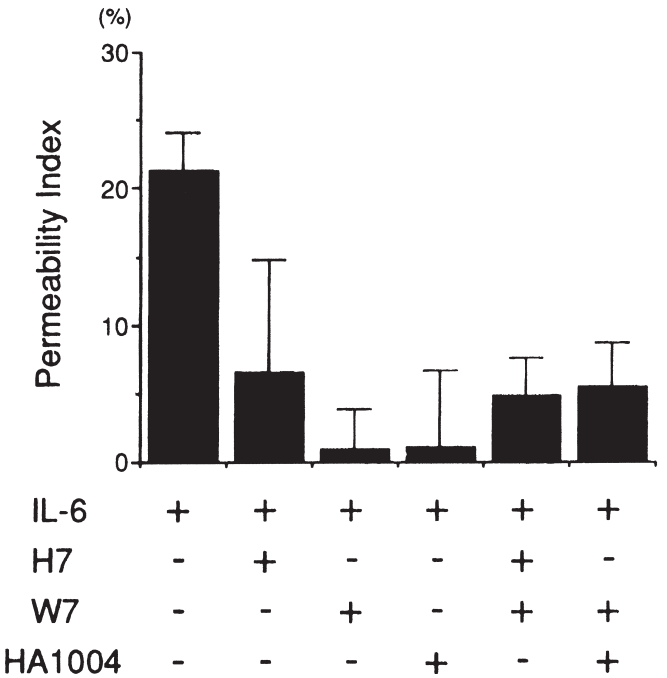

Fig. 31 Effect of protein kinase inhibitors, H7 and HA1004, and a calmodulin antagonist, W7, on albumin permeability across HUVEC monolayer by 500 U/ml of IL-6.

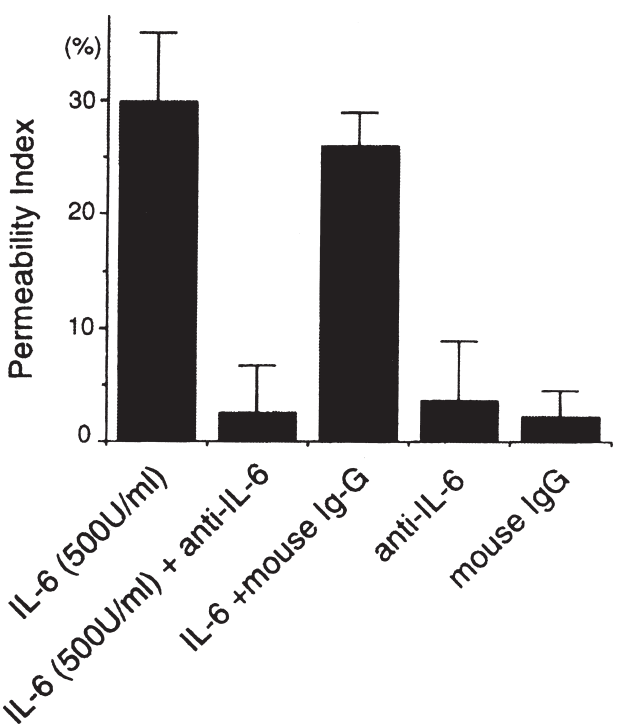

Fig. 32 Specific absorptional activity of ant-IL-6 antibody. The mouse IgG was used as a control.

11. Metastasis to the liver correlates with production of IL-6 by PCI cell lines

We next examined the *in vivo* effects of pancreas cancer-derived IL-6 and the mechanism of such action, by using 2 kinds of immunodeficient hosts; first, nude mice, which are T cell-deficient, but with a relative sparing of B cell immunity (47), and, second, SCID beige mice, which are deficient in both T and B cell immunity. The genetic background of these mice is otherwise similar. PCI-6, 10, 19, 24, 35, 43, 55, 64, and 66 have been examined earlier for their potential for *in vivo* liver metastasis (37). We evaluated the possible correlation between the number of metastatic liver nodules and their potential to secrete IL-6 into the culture medium. Production of IL-6 has been detected by ELISA and by northern hybridization in PCI-6, 10, 19, and 35 but not in PCI-24 or 43, in another study (41). Since we considered that the production of IL-6 might relate to the metastatic phenotype, we examined the concentrations of IL-6 in the supernatants of 9 PCI lines. The metastatic phenotype exhibited by PCI lines inversely correlated with IL-6 production ($p<0.001$) (Fig. 33). Although most of the data presented in Figure 33 were from our earlier studies, these data highlight a previously undetected correlation, which prompted us to undertake subsequent experiments.

12. Human IL-6-cDNA-transfected PCI-43 subclones and their characterization

We introduced an IL-6-producing phenotype into an IL-6-non-producing PCI-43 line by using BCMGneo-hIL-6 cDNA. We obtained 12 colonies in G418-containing culture media, and 5 clones were randomly selected for evaluating IL-6 production. The 5 PCI-43 subclones produced 0 to 5080 pg/ml of IL-6 in 48 hr-culture media. Three out of 5 subclones and the original (parent) PCI-43 were used for subsequent studies. Subclones PCI-43h (high-producer), PCI-43l (low-producer), and PCI-43n (non-producer) produced IL-6 at concentrations of 5080, 60.7, and 0 pg/ml, respectively. All 3 subclones had a morphology identical to that of parent PCI-43 cells in culture. Production of IL-6 by PCI-43h and 43l was maintained for at least 2

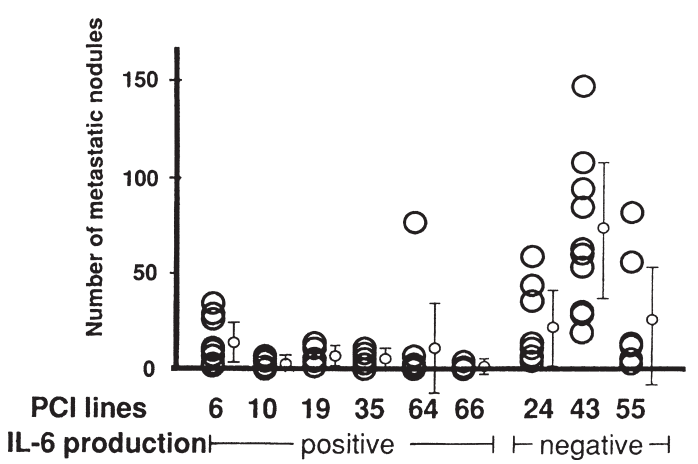

Fig. 33 Correlation of metastatic phenotype and IL-6 production in PCI lines.

months *in vitro*.

The values of doubling time of parent PCI-43, 43h, 43l, and 43n *in vitro*, as determined by the WST-1 assay, were 20.2±1.3, 18.9±3.4, 20.2±3.0, and 22.9±8.8 h, respectively. Expression of surface molecules was almost identical, with only minor variations (Table 3). Expression of surface receptor for IL-6 was not detected in any of parent and transfected subclones. Addition of 1000 U/ml of human IL-6 did not modulate the doubling time of parent PCI-43 (19.5±0.4 h). The subclone PCI-43l exhibited slightly increased kinesis ($p<0.01$) (Fig. 34). Subclones otherwise showed no significant alterations in kinesis and invasiveness (Fig. 34). None of the parent and transfected PCI-43 subclones was susceptible to NK cytotoxicity at effector-to-target (E:T) ratios ranging from 12.5 to 100. Only the positive control line, K562, was susceptible to NK cytotoxicity, percent cytotoxicity being 0, 24.6±9.8, 29.1±25.8, and 23.9±22.4, at E:T ratios 12.5, 25, 50, and 100, respectively.

Table 3 Expression of surface molecules in parent and IL-6-transfected PCI-43 sublines.

Surface molecules[2]	Parent PCI-43	PCI-43n	PCI-431	PCI-43h
A-ABC	+	+	+	+
HLA-DR	−	−	−	−
CEA	+	±	+	+
IL-6 receptor	−	−	−	−
VLA-5	−	−	−	±
VLA-6	−	−	−	−
Mac-1	−	−	−	−
E-selectin	−	−	−	−
Sialyl Lewis^x	±	±	±	±
Sialyl Lewis^a	+	+	+	+
ICAM-1	+	+	+	+
ICAM-2	+	+	+	+
LFA-3	+	+	±	±

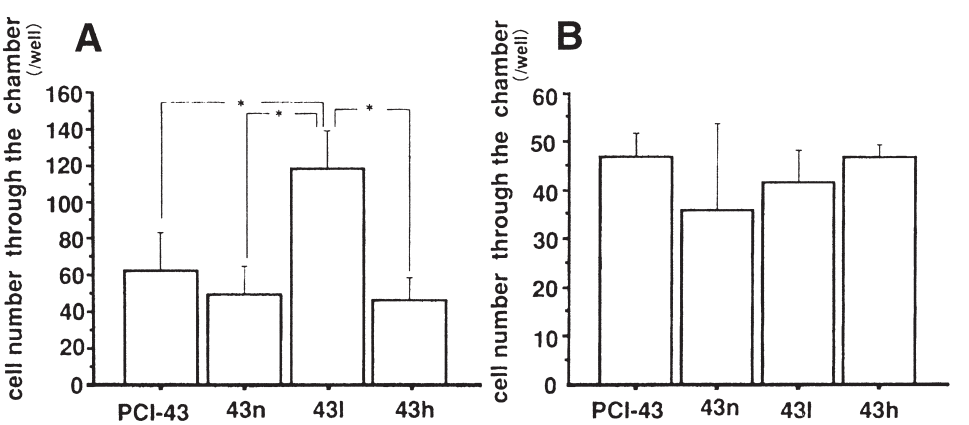

Fig. 34 Kinetics (**A**) and invasiveness (**B**) *in vitro* in parent and IL-6-transfected PCI-43 sublines. *: $p<0.01$.

13. Potential of IL-6 cDNA-transfected PCI-43 subclones for liver metastasis

The parent and transfected PCI-43 lines were examined for their potential for blood-borne metastasis to the liver by injecting tumor cells into the spleen of nude mice. The number of metastatic liver nodules per unit liver volume was calculated using the formula of Enzmann *et al*. (39). The parent PCI-43 cells generated 193.5±169.1 colonies/cm³ liver volume, and the numbers of PCI-43n, 43l, and 43h were 84.1±99.3, 409.3±328.3, and 27.0±33.1 colonies/cm³, respectively (Fig. 35). The number of metastatic nodules in PCI-43h was significantly lower than those of parent PCI-43 ($p<0.01$) and PCI-43l ($p<0.01$). There was no statistically significant difference between PCI-43h and PCI-43n, although a trend for suppression of metastasis in PCI-43h was noted. The parent PCI-43, PCI-43n, PCI-43l, and PCI-43h generated tumor nodules in the injected spleen, the numbers of splenic nodules being 26.9±46.2, 36.7±35.1, 23.6±35.8, and 25.6±43.9 colonies/cm³, respectively. We found no metastatic tumor nodules in any organ other than the spleen and liver. There were no significant alterations in histopathologic features of metastatic nodules of these 4 PCI lines; they were mostly poorly differentiated adenocarcinoma with sparse formation of neoplastic tubules and production of mucin.

14. Detection of human IL-6 and tumor-reactive IgG and IgM in nude mouse sera

We measured human but not murine IL-6 species by ELISA, and observed the presence of human IL-6 in nude mouse sera xenotransplanted with PCI-43h cells only (40.6±37.4 pg/ml). IL-6 was undetectable in sera from parent PCI-43-, PCI-43n-, and PCI-43l-inoculated, and naive nude mice. The amounts of human IL-6 in sera of PCI-43h-inoculated mice correlated with numbers of metastatic colonies in the liver ($p<0.01$) (Fig. 36), indicating that PCI-43h cells produced and secreted human IL-6 *in vivo*. Nude mouse sera were then examined for the presence of

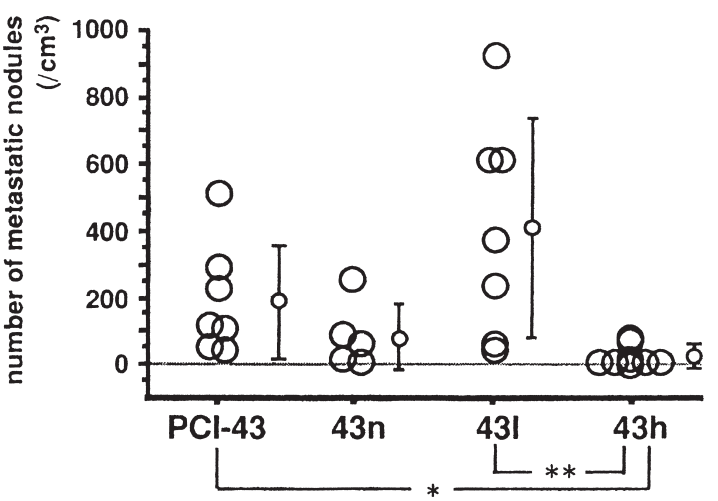

Fig. 35 Metastatic potentials of parent and IL-6-transfected PCI-43 sublines in nude mice. * and **: $p<0.01$.

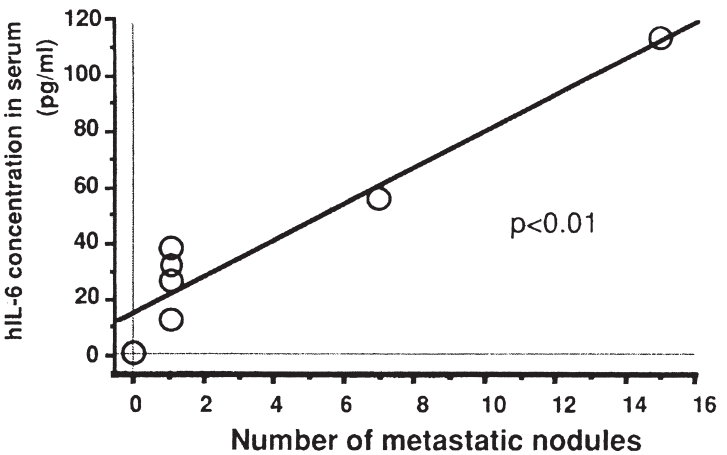

Fig. 36 Correlation of serum IL-6 concentration and the number of metastatic nodules in the liver in PCI-43h-inoculated mice ($p<0.01$).

immunoglobulins reactive with inoculated PCI-43 species by indirect flow cytometry. Tumor-reactive IgG was demonstrated only in sera from recipients of PCI-43h inoculation, while it was not seen in sera from mice inoculated with parent PCI-43, 43l, or 43n, except for a PCI-43l-inoculated mouse ($p<0.05$) (Fig. 37). Tumor-reactive IgM was detected in sera from all recipient mice, which we interpreted as being a natural antibody because naive nude mouse sera also contained similar amounts of parent PCI-43-reactive IgM. A slight augmentation, however, in tumor-reactive IgM was seen only in sera from 2 of 6 PCI-43h-inoculated nude mice.

15. ADCC activity mediated by tumor-reactive immunoglobulins in PCI-43h-inoculated nude mice

Two of 6 sera samples from recipients of PCI-43h nude mice were evaluated for

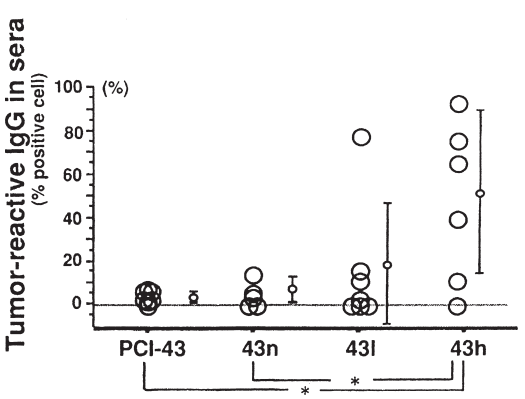

Fig. 37 Amounts of tumor-reactive IgG in sera from nude mice inoculated with the parent or IL-6-transfected PCI sublines. The amount of each mouse is shown by percent of positively stained PCI-43. *: $p<0.01$.

ADCC. One of 2 sera that contained tumor-reactive IgG in a high titer, exhibited a slight ADCC activity, whereas the other that contained IgG in a lower titer did not (Fig. 38).

16. Subcutaneous injection of a suboptimal dose of PCI cells in nude and SCID mice

All PCI lines, including parent PCI-43 cells, can generate tumor nodules in nude mice, when injected s.c. with $1x10^7$ cells/0.5 ml PBS. We performed experiments in which a suboptimal dose of PCI cells, *i.e.*, $1x10^6$/0.1 ml PBS, was inoculated s.c. into BALB/c *nu/nu* and SCID beige mice. The parent PCI-43, 43l, and 43n cells did not generate tumor nodules throughout the course of observation (up to 29 days), as expected from our previous data. The PCI-43h cells inoculated into nude mice yielded at first, discernible small nodules, maintained their tumor size for some time, and finally became indiscernible. In interesting contrast, when the PCI-43 series was inoculated into SCID beige mice, the parent PCI-43, 43l, and 43n did not grow to a discernible size as in nude mice, but PCI-43h grew to produce established nodules (Fig. 39). When mice were killed and nodules were observed histologically, the s.c. nodules were composed of PCI-43h cells with scattered necrotic foci. Tumor-reactive IgG or IgM was not seen in sera from these SCID beige mice.

17. Summary and perspectives

Cellular adhesion of SLe^a-positive pancreatic carcinoma to endothelial cell (EC) is augmented by activation of EC via an upregulated E-selectin expression on EC. Co-cultivation of PCI-24, with HUVEC for 5 h at the PCI-to-HUVEC ratio of 1:10

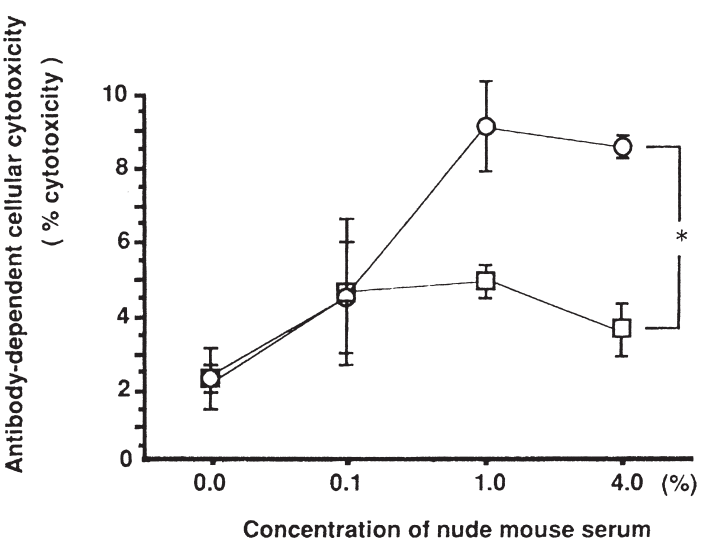

Fig. 38 Antibody-dependent cellular cytotoxicity mediated by sera of nude mice inoculated with PCI-43h. Results of sera contained the high titer (○) and the low titer (□) of tumor-reactive IgG are shown.

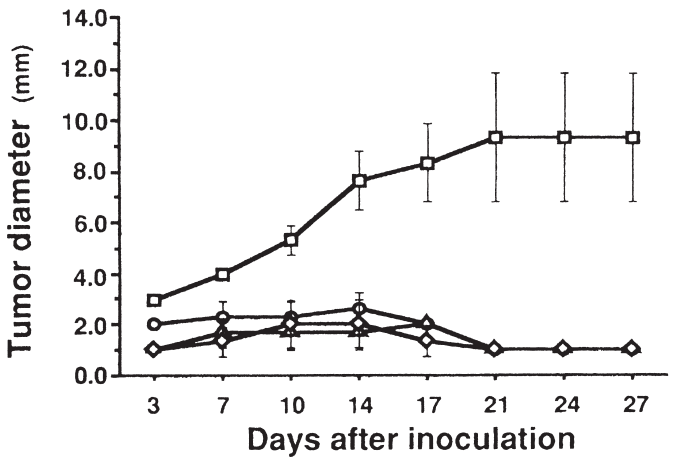

Fig. 39 Tumor growth in SCID beige mice injected with parent or IL-6-transfected PCI-43 sublines, at suboptimal dose (1 X 10^6 cells/0.1 ml PBS) for the consistent establishment of tumor nodules. ○: parent PCI-43, ◇: PCI-43n, △: PCI-43l, □: PCI-43h.

induced E-selectin expression on the endothelial cell surface, augmenting SLe^a-positive pancreatic carcinoma cell attachment with HUVEC. Culture supernatants of six PCI cell lines contained soluble, E-selectin-inducing factor(s). The E-selectin-inducing effect by the supernatants was blocked by the protein kinase C inhibitor, H7. Antibodies against SLe^a and E-selectin but not SLe^x or ICAM-1 blocked the increased pancreatic carcinoma-to-endothelial attachment. PFA-fixed PCI-24 cells also induced E-selectin on vascular endothelial cells upon direct contact with endothelial cells, indicating the presence of a membrane-bound form. The six PCI cell lines all produced IL-1α mRNA and protein but not IL-1β or TNF-α protein and/or mRNA. Absorption of IL-1α from the supernatants by IL-1α-specific antibody almost completely abolished the E-selectin-inducing activity. Anti- IL-1α antibody also abolished the E-selectin-inducing activity of PFA-fixed PCI. IL-1α production by PCI cells was upregulated by TNF-α. These observations suggest that substance(s) produced by pancreatic carcinoma cells, in this case, IL-1α, may contribute to pancreatic carcinoma cell colonization in non-inflamed, distant locations *in vivo*, by activating vascular endothelial cells. Culture supernatant of PCI-10, but not PCI-24, induced an augmented albumin permeability across the EC monolayer, an event which was blocked by the calmodulin antagonist, W-7. Only marginal inhibitory effects were obtained using protein kinase inhibitors, H-7 and HA-1004. When cytokine production by pancreatic carcinoma cells was examined, production of IL-6 in large amounts by PCI-10, but not by PCI-24 cells was evident. As recombinant IL-6 generated a dose-dependent permeability increase, and as this effect was inhibited by W-7, it was shown that the enhancement of vascular permeability was mediated by this cytokine. The activity of culture supernatants for enhanced permeability was almost completely absorbed by the addition of an antibody specific for IL-6. Tumor-derived IL-6 as

a soluble mediator regulates vascular permeability *in vitro*. Production of IL-6 by human pancreatic carcinoma cells inversely correlated with potentials for blood-borne metastasis to the liver in nude mice. IL-6 cDNA was transfected to PCI-43, one of PCI cell lines that does not produce IL-6 and generates numerous metastasis to the liver. As an IL-6-high producer clone (PCI-43h) generated few metastasis, IL-6 production has a direct effect on metastasis, whereas other transfectants (PCI-43l and PCI-43n), did generate metastases. Tumor-reactive IgG, which mediated an activity for ADCC *in vitro*, was detected in sera from recipient nude mice inoculated with PCI-43h but not in those given PCI-43l, PCI-43n, or parent PCI-43. Tumor-reactive IgM was detected in sera from all mice, irrespective of inoculated PCI-43 species, with a slight augmentation being noted in PCI-43h-inoculated nude mice. SCID beige mice were then used as recipients for PCI-43 species, and tumorigenesity was examined by s.c. inoculation of a suboptimal number of PCI-43 transfectants ($1x10^6$/0.1 ml). Only PCI-43h formed palpable masses in SCID beige mice, whereas it first grew to be palpable but subsequently became not palpable in nude mice, thereby revealing the dual action of tumor-derived IL-6. Thus, tumor-derived IL-6 confers growth promotion in SCID beige mice, while the same cytokine exhibits anti-tumorigenic functions, presumably through humoral immune responses, in nude mice. Finally, whether and how carcinoma-producing cytokines, IL-1α and IL-6 described here play significant biological roles *in vivo* in patients will remain to be determined.

Anti-angiogenic Agent, TNP-470, and Hematogenous Cancer Metastasis (48, 49)

1. Introduction

The prognosis of patients with pancreatic carcinoma is morbid and major causes of death are either metastasis of this lesion to the liver or peritoneal dissemination. Metastases to the liver, present in postoperative patients are not often apparent prior to surgery, or intraoperatively. Therefore, treatment to inhibit micrometastases should be considered. Growth of micrometastasis to a clinically detectable size requires neovascularization (50). Therefore, if the angiogenesis of micrometastasis could be controlled, an improved clinical state could be expected. Among angiogenesis inhibitors, O-(chloroacetyl-carbamoyl) fumagillol (TNP-470) has received attention because of its antitumor effects. TNP-470 is a derivative of fumagillin, an antibiotic naturally secreted by Aspergillus fumigatus fresenius; it inhibits proliferation of endothelial cells at concentrations that are not suppressive for tumor cell growth (51). In addition, TNP-470 inhibits growth and metastasis of several types of human (52–54) and animal (55–57) tumors *in vivo*. However, vascularization in primary and metastatic tissues varies, depending on phenotypes of tumor cells, and generalization of anti-angiogenic effects of a given drug is hindered. To examine effects of TNP-470 against hepatic metastasis of a pancreatic cancer cell line, we used T-, B-, and NK-deficient, SCID beige mice, the

objective being to exclude any possible interference by the immune system. Although the importance of tumor angiogenesis has been widely accepted in the case of blood-borne metastases, its importance in the establishment and growth of peritoneal dissemination remains largely unknown (58). The peritoneal implants of pancreatic adenocarcinoma patients histologically are composed of a proliferation of carcinoma cells accompanied by desmoplastic stromal reaction with neovascularization. Thus, inhibition of tumor angiogenesis might suppress peritoneal implants, as in the case of hematogenous metastatic nodules (48, 59–61). We established and characterized dissemination-prone subcultures of a pancreatic adenocarcinoma cell line to examine whether TNP-470 treatment, a known effective therapy for blood-borne metastasis, would be a beneficial treatment against peritoneal dissemination.

2. Metastasis to the liver

The number of metastatic colonies per unit liver volume was calculated, using data on the number and radius of metastatic colonies detected microscopically. Compared with control groups, the number of liver metastatic colonies per unit volume (/cm^3) was reduced in TNP-470-injected mice in both 6- and 10-week administered groups ($p=0.241$ and $p=0.073$, respectively) (Fig. 40). The mean values of control groups (370.96 ± 284.72 vs. 196.92 ± 99.09), as well as those of TNP-470-treated groups (23.16 ± 8.75 vs. 35.97 ± 24.61), did not differ between animals in the 6- and 10-week-experiments. Regarding the average of the largest diameter of colonies in each mouse, no inhibitory effect on size of the colonies was observed in the 6-week-experiment, but a tendency toward suppression was seen in the 10-week-experiment (Fig. 41). As metastatic nodules were present in only 2 of

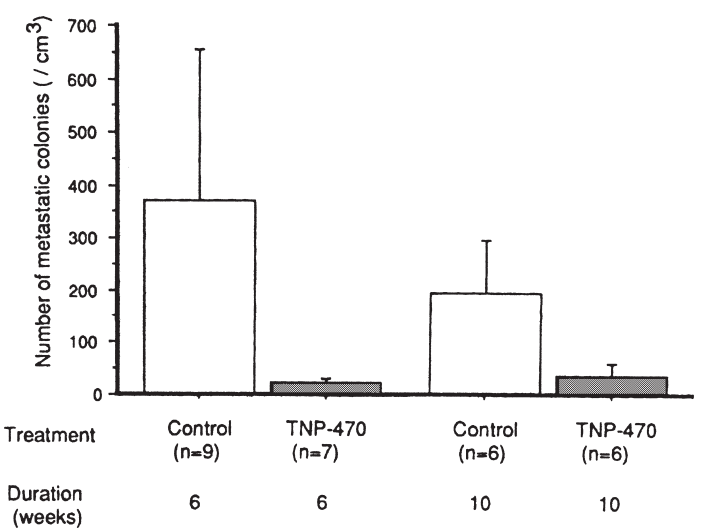

Fig. 40 Inhibitory effect of TNP-470 on the number of metastatic colonies per unit volume of the liver from SCID beige mice injected PCI-43.

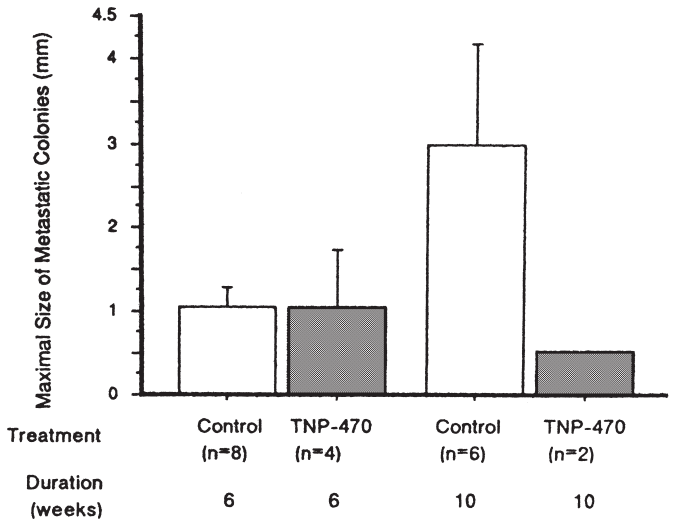

Fig. 41 Inhibitory effect of TNP-470 on the average size of the largest metastatic colony in each mouse injected PCI-43.

6 mice in the TNP-470-treated group in the 10-week-experiment, statistical analysis was not feasible. No difference was observed between TNP-470 administered mice and control mice on liver weight per mouse body weight (0.067 ± 0.0045g vs. 0.060 ± 0.0040 g in the 6-week group, 0.065 ± 0.0071g vs. 0.068 ± 0.0065g, respectively). Body weights of mice during the experiment were measured. In both 6- and 10-week-experiments, loss of weight occurred in TNP-470-administered mice (statistically not significant in the 6-week group, and $p < 0.01$ in the 10-week one), while control groups gained weight.

3. Proliferation and apoptosis of metastatic colonies

Proliferating cell nuclear antigen (PCNA) and TUNEL stains were applied to metastatic colonies (Fig. 42). The percentage of positively stained tumor cell nuclei was defined as PCNA and apoptotic indices, respectively. In the TNP-470 group treated for 6 weeks, the PCNA index was suppressed and the apoptotic index increased significantly (each, $p < 0.05$). This was reproduced in the 10-week-experiment (each, $p < 0.01$). Thus, TNP-470 induced inhibition of cell proliferation and acceleration of apoptosis in colonies of metastases in the liver.

4. Cell proliferation assay *in vitro*

The growth of HUVECs cultured with TNP-470 was significantly inhibited with each concentration ($p < 0.01$). The inhibitory effect was in a dose-dependent manner at concentrations below 100 ng/ml (Fig. 43). On the other hand, inhibitory effects were nil regarding growth of PCI-43 cells, at any concentration with which growth of the HUVEC was inhibited.

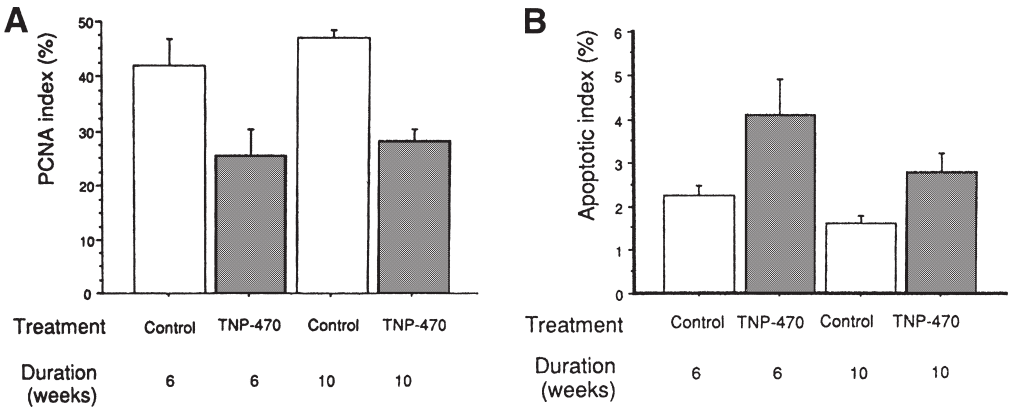

Fig. 42 Effects of TNP-470 on proliferation (**A**) and apoptotic cell death (**B**) of metastatic PCI-43 cells in the liver.

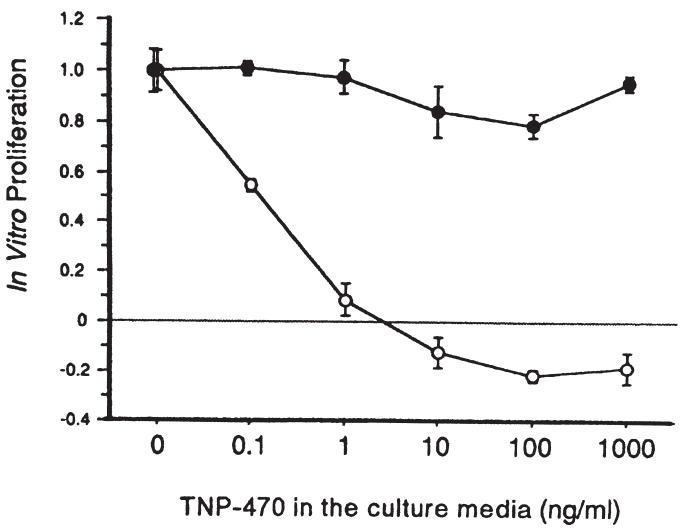

Fig. 43 Effect of TNP-470 on *in vitro* proliferation of HUVEC (○) and PCI-43 (●).

5. Angiogenesis induced by PCI-43 *in vivo*

The neovascularization induced by PCI-43 on subcutaneous tissue contiguous to fascia of SCID beige mice was suppressed in TNP-470 administered mice.

6. Establishment of dissemination-prone PCI-43 subcultures

Peritoneal dissemination was only rarely found in the original PCI-43 culture, while the PCI-43 subcultures were able to establish peritoneal implants. The numbers of established nodules increased with *in vivo* passage in the peritoneum, with PCI-43p3 cells being superior to any other subculture. The dissemination nodules were composed of carcinoma cells and stromal fibroblasts and capillaries. No ascites was observed in PCI- and its subculture-inoculated mice.

7. Characterization of *in vivo* selected dissemination-prone PCI-43p3

Zymographic examination revealed that the 92 kDa matrix metalloproteinase (MMP)-9 was expressed *in vivo* selected PCI-43p3 but not in conditioned supernatants from the original PCI-43 culture. No obvious activated form of MMP-9 was seen in either PCI-43 or PCI-43p3 supernatants. In contrast, the 72 kDa MMP-2 was expressed in supernatants from both cultures. No obvious activated form of MMP-2 was seen in either PCI-43 or PCI-43p3 supernatants. The culture supernatants from PCI-43 and PCI-43p3 produced vascular endothelial growth factor (VEGF) at concentrations of 231 ± 3 and 470 ± 42 pg/ml, respectively ($p<0.005$). The RT-PCR revealed that the two types of splicing variants, $VEGF_{121}$ and $VEGF_{165}$, were detected in the original and all subculture PCI cells. There was no apparent alteration in the relative density pattern of the two kinds of amplified product. Flow cytometry revealed that the PCI-43 subcultures, PCI-43p1, p2, and p3, all exhibited surface expressions of ICAM-1, VLA-3 and E-cadherin, and no difference was seen among these PCI cells.

The attachment assay revealed no significant adhesion between cultured mesothelial cells and PCI-43, PCI-43p1 or PCI-43p2 cells. In contrast, a pronouncedly augmented attachment was seen between mesothelial and PCI-43p3 cells, which was not affected by the addition of TNP-470 into the medium at concentrations of 0.1, 1, 10, 100, and 1000 ng/ml.

8. Suppression of *in vivo* growth of peritoneal implants by the anti-angiogenic TNP-470

Numbers of mesenteric nodules were reduced in the TNP-short-treatment (9.4 ± 2.1) and TNP-long-treatment (1.8 ± 1.3) groups, compared with the control group (21.0 ± 6.9) ($p<0.01$, control vs. TNP-short-treatment; $p<0.0002$, control vs. TNP-long-treatment group). The reduction of nodule numbers was more extensive in the long-treatment than the short-treatment group ($p<0.0002$). The largest nodule diameters (mm) were smaller in the TNP-treatment groups (control, 5.4 ± 1.0; TNP-short-treatment, 3.2 ± 1.3; TNP-long-treatment, 1.0 ± 0.7) ($p<0.007$, control vs. TNP-short/long-treatment groups), and the suppression was more extensive in the long-treatment than in the short-treatment group ($p<0.02$). The PCNA indices for the control, TNP-short-treatment, and TNP-long-treatment groups were 75.3 ± 7.7, 49.7 ± 9.0 and 52.7 ± 10.4, respectively ($p<0.003$, control vs. TNP-short/long-treatment groups). Body weight gain (g) in each group was 2.9 ± 1.6, 2.9 ± 1.0 and 0.2 ± 1.0 for the control, TNP-short-treatment, and TNP-long-treatment groups, respectively ($p<0.05$, control vs. TNP-long-treatment group; $p<0.02$, TNP-short-treatment vs. TNP-long-treatment group).

9. Summary and perspectives

TNP-470 on hematogenous metastasis of a human pancreatic carcinoma cell line were examined. One$\times10^6$ cells of PCI-43, a human pancreatic carcinoma cell

line were injected into the spleen of SCID beige mice, then TNP-470 at 30 mg/kg was administered subcutaneously every other day. The mice were killed 6 or 10 weeks thereafter and metastatic nodules in the liver were counted and measured microscopically. Metastases were inhibited and about a 10% loss of weight was evident in the TNP-470-administered mice. There was no suppression in maximal size of metastatic colonies in mice given the agent for 6 weeks, while inhibition was apparent in mice given the drug for 10 weeks. Suppression of cell proliferation and increase of apoptosis were evident in metastatic nodules in the TNP-470-administered groups. TNP-470 inhibited the proliferation of HUVEC but not PCI-43 *in vitro*. TNP-470 did not suppress production of VEGF by PCI-43 cells. Neovascularization *in vivo* induced by PCI-43 was suppressed in the TNP-470-administered mice, using a diffusion chamber placed in subcutaneous tissues of SCID beige mice. These observations suggest that inhibition of angiogenesis is effective in suppressing establishment and subsequent growth of hematogenous micrometastases of pancreatic adenocarcinoma to the liver. Next, we established peritoneal dissemination-prone subcultures (PCI-43p3) using nude mice by a repetitive *in vivo* selection of intraperitoneally inoculated PCI-43. The subcultures showed upregulated expression of MMP-9 but not MMP-2 in culture supernatants. They also produced increased amounts of VEGF, which was not associated with alterations in isoforms of VEGF mRNA. PCI-43p3 cells attached with cultured mesothelial cell monolayers incrementally compared with the parent PCI-43 cells. The angiogenesis inhibiting agent, TNP-470, was administered to the model mice, resulting in a prominent suppression of the establishment of peritoneal nodules. The suppression was dependent on the duration of TNP-470 treatment. TNP-470 treatment significantly suppressed proliferation of tumor cells in disseminated nodules when assessed by immunostaining for PCNA. TNP-470 did not affect the *in vitro* attachment between PCI-43p3 and mesothelial cells. The combined data show that anti-angiogenic treatment profoundly suppresses the *in vivo* process of peritoneal dissemination.

Prediction of Prognosis of the Patients with Solid Cancers by Gene Expression Profiling

1. Introduction

A growing body of knowledge on the molecular biological aspects of cancer has been revealing the interlacing, complex mechanisms of carcinogenesis and multistep progression of cancers, involving many genes such as oncogenes, tumor suppressor genes, cell cycle regulatory genes, apoptosis-related genes and those of growth factors, intercellular adhesion molecules and catabolic enzymes (62, 63). Accordingly, it is considered difficult to attribute a malignant property of cancer to an abnormality of a single gene. Apart from such a singular gene-oriented approach, expression profiling that collectively analyzes expressions of many genes

using of cDNA array has drawn an attention as a promising approach to uncover molecular mechanisms independently of previous knowledge (64). It is, however, a difficult task to extract truly significant information characteristic to a biological property from noisy and messy data of thousands dimension. To date, a number of methods for mining up gold from array data have been reported, including unsupervised approaches such as cluster analysis (65) and self-organizing map (66) and supervised learning machines such as neural network (67, 68) and support vector machine (69, 70), with or without dimensional reduction by principal component analysis(projection pursuit) (71), singular value decomposition (72), and feature subset selection (73–75).

In this section, we analyzed expression profiles in a total of 89 cases of colorectal carcinoma, 27 cases of panceas carcinoma and 54 cases of gastric carcinoma (manuscripts in preparation).

2. Colorectal carcinoma

Accurate preoperative prediction of lymph node metastasis and degree of tumor invasion would facilitate an appropriate selection in extent of surgical resection of cancers, reducing unnecessary cost of complication or minimizing risk of recurrence in patients. We analyzed gene expression profiles characteristic to invasiveness of colorectal carcinoma on a total of 89 cases using of a cDNA array and pattern classification algorithms. We set binary classes for a panel of clinicopathologic parameters each of which was divided at different levels of categories (discrete) or values (continuous). For each pair of classes, preselection of genes were performed on the basis of statistical difference in mean expressions between classes (two-sided t-test, $p \leq 0.05$). From these starting sets of genes, we searched an optimal combination of genes to discriminate classes using of a feature subset selection algorithm. We employed a sequential forward feature selection which additively search a combination of genes giving a minimal leave one out classification error rate of a k-nearest neighbor classifier. At the process of gene preselection, we found a remarkable difference in expression pattern of genes according to the anatomical location of cancers. The difference was the most prominent when the classes were set for cecum, ascending colon, transverse colon, and descending colon versus sigmoid colon and rectum. By stratifying these two locations, we were able to extract gene expression profiles characteristic to classes for the presence versus absence of lymph node metastasis, lymphatic invasion, and vascular invasion and degree of mural invasion, and pathological stages, with an accuracy of more than 90%. These results suggest that colorectal cancers harbor distinct molecular pathophysiological statuses according to their right-to-left locations, of which stratification is important for pattern classification of cDNA array data.

3. Pancreatic carcinoma

We investigated gene expression profile that characterizes and predicts the risk in survival of patients with pancreatic carcinoma, examining the cDNA array data obtained from a total of 27 pancreatic carcinoma tissues. For validation of the predictive models, we first took randomly selected 6 cases out of the 27 cases, and trained a k-nearest neighbor classifier with the remaining 21 cases. After preselection of 47 genes differentially expressed between the classes, we performed a supervised sequential forward selection which identified sets of genes optimal for pattern classification by evaluation of leave one out error of k-nearest neighbor classifiers. We could select a maximum of 44 genes which gave 100% prediction of the patients outcome. We formed an ensemble learning classifier combining the 39 models with each vote weighted by Bayesian posterior probabilities of misclassification. This ensemble classifier performed a 100% accuracy in a 60 times internal cross validation tests. A cross-validation test on the 6 left test cases correctly predicted the outcomes in 5 of 6 cases, demonstrating the generalization ability of the classifier. On the other hand, we tested all the 1289 genes for correlation to the patients' survival periods with generalized Wilcoxon test. We found a correlation to survival of 83 genes of which 9 were common with the above 47 genes ($p=0.00035$). A contingency table analysis on the available clinicopathological factors revealed a trend of correlation of patients survival with the histological grading and serum CA19-9 levels. Some of the differentially expressed genes for these parameters were common with the 47 genes but many of them were distinct, suggesting that the risk in survival in pancreatic cancer patients can be partly but not all attributable to the two factors. Taken together, we infer the feasibility of cDNA array data-based prediction of risk in short time survival with the presently established method of analysis.

4. Gastric carcinoma

We assessed the predictability of various classes defined by clinicopathological parameters including invasiveness and clinical outcomes of gastric carcinoma using of cDNA array data obtained from a total of 54 cases. We set two-level classes for the parameters each of which was divided at different levels of categories (discrete) or values (continuous). For each pair of classes, we preselected genes on the basis of statistical difference in mean expressions between classes (two-sided t-test, $p \leq 0.05$). Out of these starting sets of genes, we searched an optimal combination of genes giving to discriminate classes using of a feature selection which additively search a combination of genes giving a minimal leave one out classification error rate of a k-nearest neighbor classifier. By these procedures we could successfully selected sets of genes on which the classifier predicted better versus worse overall survival (tumor specific death) and tumor free survival (recurrence), with respective classification rate of 94% and 92%. A contingency table analysis (χ^2-test) and Cox' proportional hazard model analysis revealed lymph node metastasis is the most

important factor (confounding factor) related with the patients' prognosis and risk of recurrence. The feature subset selection procedure successfully extracted expression patterns characteristic to the presence versus absence of lymph node metastasis and lymphatic vessel invasion, yielding the accuracies of prediction of 92% and 98%, respectively. These results suggest that invasiveness of a gastric carcinoma is the most important target of prediction based on expression profiling to know the prognosis of the patient. We also suggest that accurate preoperative prediction of the invasiveness of gastric carcinoma by the presently established method would facilitate the optimal selection of extent of surgical resection and use of adjuvant therapy, which minimize both the cost of complication and risk of recurrence.

Immunotherapy and Gene Therapy against Cancers

In this section, three different research works for immuno- and gene therapy against cancers will be presented. First one is to use IL-6 producing carcinoma to generate IgG antibody response against carcinoma cells. Second is to use fusion cells between dendritic cells and carcinoma cells for active vaccination for cancer, and the third is gene therapy using AFP enhancer/promotor-specific transfer of the herpes siniplex virus thymidine kinase (HSVtk) gene followed by ganciclovir (GCV) administration for particular carcinoma, AFP producing hepatoid adenocarcinoma.

1. Vaccination effect of IL-6-producing PCI cells in nude mice: A model of tumor prevention and treatment in immune compromised patients (76)

1) Introduction

Tumor-derived cytokines, especially IL-6, can convey variable functions such as proliferation of tumor cells in an autocrine fashion (77), local permeability increase (41), and stimulation of host immunity (42). Importantly, an IL-6-mediated anti-metastatic effect in mice has been shown in colon cancer (78) and in pancreatic cancer (42), providing hope for an IL-6-mediated tumor vaccination. However, other studies failed to show the effectiveness of the procedure (79). The ambiguity may have resulted from the heterogeneity of host immune status and/or from the heterogeneity of antigenicity of tumor cells. Addressing these issues appears to be important in light of the possibility of applying the cytokine-based tumor vaccination to patients. Any anti-tumor or vaccination effect that can be achievable in immune-compromised hosts is important, because of possible immune suppression resulting from chemotherapy for cancer patients. Since a T-cell deficiency with a relative preservation in B-cell function is a usual outcome of immunosuppressive treatment for patients (80), a cytokine-based vaccination against thymus-independent tumor antigens should be considered.

Our previous studies have focused on IL-6 because the production of this cytokine reversely correlates with blood-borne metastasis of pancreatic adenocar-

cinoma cells in T-cell-deficient nude mice (42). Transfection of IL-6 cDNA into metastasis-prone, IL-6-negative PCI-43 cells dramatically altered their phenotype into a non-metastatic one without changing either *in vitro* proliferation or ability for invasion (42). Furthermore, a spontaneous regression occurred in tumor xenografts composed of IL-6-producing transfectant cells (42). Interestingly, no regression has been observed in T/B-cell-deficient SCID mice, implying that the immune status of the host greatly affects the action of tumor-derived IL-6 and that the regression was probably mediated by humoral immune response. Circulating IgG antibodies, which had an *in vitro* activity of ADCC (42), have been detected in nude mice that apparently rejected human pancreatic adenocarcinoma xenografts. The IgG antibodies were not seen in mice sera injected with IL-6-nonproducing PCI-43 (42). The present study, in this context, attempts further analysis, focusing especially on the specificity and kinetics of the IgG and on a possible vaccination effect in the T-cell function-deficient animal model.

2) Specificity of serum IgG

Table 4 summarizes the specificity of IgG that were affinity-purified from IL-6-producing PCI-43h-bearing nude mice sera, which were taken 4 weeks after the inoculation of $1x10^6$ PCI-43h. A fraction of the pancreatic adenocarcinoma cell lines, PCI-6, -10, and -43 expressed surface antigen(s) that react with the IgG; but the other cell lines, PCI-19, -24, -55, -64, -66, -68, -72, and -79 did not. In addition, OSRC-2, a renal cell carcinoma line; MKN-28, a stomach carcinoma cell line; and Takigawa, an α-fetoprotein-producing gastric cancer cell line, expressed the

Table 4 Reaction of serum IgG in nude mice inoculated with IL-6-producing PCI-43h.

Cell line	Origin	Reaction with serum IgG
PCI-6	Pancreas carcinoma	±
PCI-10	Pancreas carcinoma	+
PCI-19	Pancreas carcinoma	−
PCI-24	Pancreas carcinoma	−
PCI-43	Pancreas carcinoma	+
PCI-55	Pancreas carcinoma	−
PCI-64	Pancreas carcinoma	−
PCI-66	Pancreas carcinoma	−
PCI-68	Pancreas carcinoma	−
PCI-72	Pancreas carcinoma	−
PCI-79	Pancreas carcinoma	−
OSRC-2	Renal cell carcinoma	+
MKN-28	Gastric carcinoma	±
HSC-42	Gastric carcinoma	−
Takigawa	Gastric carcinoma	+
HTOA	Ovarian carcinoma	−
SQ-5	Lung carcinoma	±
HUVEC	Umbilical vein endothelial cell	−

antigen(s). On the other hand, HSC-42, a gastric cancer line; HTOA, an ovarian carcinoma cell line; and human umbilical endothelial cell culture were negative for the antigen(s). These findings, together with our previous observation that non-specific, pre-existent tumor-reactive IgM was seen in any individual naive nude mice as natural antibodies, indicate that the IgG was not a natural antibody and that the IgG resulted from a specific immune response. The PCI-43-reactive IgG in sera of PCI-43h-bearing mice first appeared one week after inoculation, and increased its reactivity during the second and third weeks. The peak reactivity was observed at the fourth week (Fig. 44), and it remained high at the sixth week.

3) Suppression of remote PCI xenografts by inoculation of IL-6-producing PCI

Our previous study demonstrated a spontaneous regression of PCI-43h xenografts, which was accompanied by the appearance of PCI-43-reactive IgG in host sera. We attempted here to see if the regression could be observed in remotely located xenografts. In addition, we examined whether or not the remote effect can be seen in PCI-24 xenografts. PCI-24 cells were used as negative controls, because they were not reactive with IgG purified from PCI-43h-bearing mouse sera. The inoculation of either PCI-43h or PCI-43 did not convey regression of control PCI-24 xenografts at the remote site. In contrast, inoculation of PCI-43h but not PCI-43 suppressed growth of PCI-43 xenografts located at the remote site ($p < 0.003$) (Fig. 45). Therefore, a regression of remote xenografts requires production of IL-6, and is specific to PCI-43.

4) Vaccination effect by pre-injection of IL-6-producing tumor

We next addressed whether or not the action of PCI-43h inoculation on the regression of PCI-43 xenografts is maintained for a certain period. For this purpose, we investigated whether or not inoculation of PCI-43h can convey a

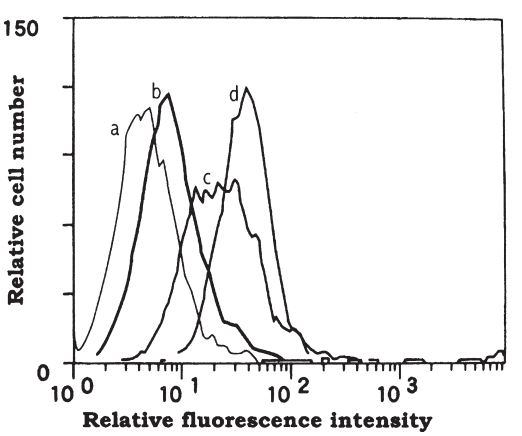

Fig. 44 Increment of tumor-reactive IgG in sera from nude mice inoculated PCI-43h. IgG purified from sera at 1 (a), 2 (b), 3 (c) and 4 (d) weeks after PCI-43h inoculation were reacted to PCI-43h, and each reaction was measured by FACS.

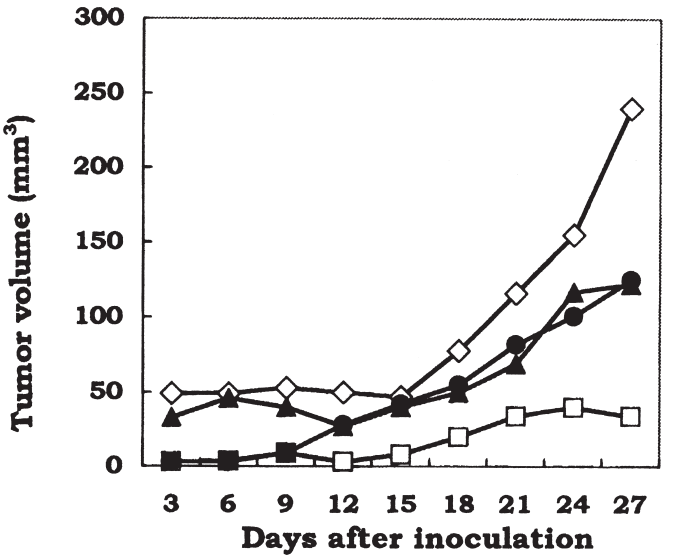

Fig. 45 Inhibition of growth of PCI-43 xenografts (open) in the right dorsum by simultaneous inoculation of PCI-43 or PCI-43h in the left dorsum of nude mice. The growth of PCI-24 xenografts (closed) in the right dorsum was examined as a control. ◇: PCI-43 (left and right), □: PCI-43h (left) and PCI-43 (right), ●: PCI-43 (left) and PCI-24 (right), ▲: PCI-43h (left) and PCI-24 (right).

suppressive effect on the growth of PCI-43 xenografts that are grafted 4 weeks later. The growth of PCI-43 was greatly suppressed when PCI-43h but not PCI-43 cells were inoculated 4 weeks earlier ($p < 0.008$) (Fig. 46), thus revealing a vaccination effect mediated by tumor-derived IL-6.

5) Summary and perspectives

In an effort to explore properties important in hematogenous metastasis of pancreatic adenocarcinoma, we previously demonstrated that tumor-derived IL-6 is a crucial factor that conveys resistance to liver metastasis. Here we extend the study to examine a possible vaccination effect of tumor-derived IL-6 in T-cell deficient nude mice, as a model for predicting the effect in immune-compromised patients. We used a pair of IL-6-nonproducing and highly producing pancreatic adenocarcinoma cell lines, PCI-43 and PCI-43h, respectively. The reaction intensity of anti-PCI IgG antibodies in host nude mice was maximal 28 days after inoculation of PCI-43h cells, and remained high thereafter. A fraction of the pancreatic carcinoma cell lines, namely, PCI-6, -10, and -43, expressed surface antigenic determinant(s) reactive with the IgG; but the others, PCI-19, -24, -55, -64, -66, -68, -72, and -79, did not. Inoculation of PCI-43h but not PCI-43 suppressed growth of simultaneously inoculated PCI-43 but not PCI-24 xenografts. In addition, administration of PCI-43h but not PCI-43 suppressed the growth of PCI-43 that was xenografted 4 weeks later, thus revealing a vaccination effect of IL-6-producing

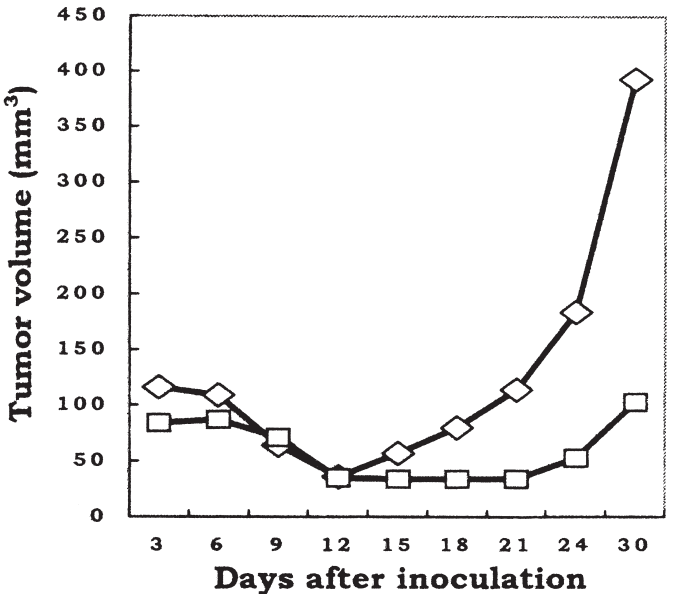

Fig. 46 Vaccination effect of PCI-43h inoculation against the growth of PCI-43 xenografts. At 4 weeks after the PCI-43h inoculation in the left dorsum of nude mice, PCI-43 was grafted in the right dorsum (□). As a control, PCI-43 was inoculated at 4 weeks before the injection of PCI-43 graft (◇).

PCI-43h but not IL-6-nonproducing PCI-43. These data, obtained from T-cell-deficient nude mice, suggest an *in vivo* role for IL-6 in inducing IgG-mediated, pancreatic carcinoma-specific vaccination against a thymus-independent antigen.

2. Vaccination of fusion cells of rat dendritic and carcinoma cells prevents tumor growth *in vitro* (81)

1) Introduction

Treatment of cancer patients with surgery, radiotherapy and chemotherapy has shown some benefits, however some types of cancer mean poor survival rates and various side effects can occur. Advances in anti-tumor immunity led to the development of more selective and safer therapeutic approaches. One such strategy is the use of dendritic cell (DC)-based vaccines. DCs are potent antigen-presenting cells capable of initiating primary immune responses (82). DCs express high levels of MHC class I, class II, co-stimulatory and adhesion molecules that provide secondary signals for stimulation of naive T cell populations (83, 84). DCs pulsed with tumor-associated peptides or proteins (85–87), and DCs transfected with genes encoding tumor-associated antigens (TAA) (88, 89) led to the induction of anti-tumor immunity. However, tumor cells may escape from immune recognition through down-regulation or alteration of single antigen and most TAAs of human tumors have yet to be identified. Thus, immunization with multiple tumor antigens, including unidentified ones, may be superior to the use of a single dominant

epitope to effectively induce anti-tumor immunity (90). Strategies so far investigated to introduce multiple antigens into DCs included DCs cultured with tumor cells (91) and DCs pulsed with tumor cell lysates (92, 93), peptides derived acid-eluates from tumor cells (94, 95) and mRNA of tumors (96, 97). Another approach to the expression of multiple and unknown TAAs on DCs is through generation of fusions between tumor cells and DCs. Recent research indicates that hybrids of tumor and DCs have been effective as vaccines for the induction of cytotoxic T lymphocytes (CTL) response and anti-tumor activity in various rodent models (90, 98–102) and in models using human materials including several clinical trials (103–106).

When we investigated fusion cells (FCs) generated from rat DCs, we found that a rat hepatocellular carcinoma cell line can effectively induce anti-tumor immunity *in vivo*.

2) Tumor cells, preparation of DCs, cell fusion and staining for phenotype

KDH-8 is a transplantable rat hepatocellular carcinoma cell line established from a tumor induced by 3'-methyl-4-dimethylaminoazobenzene in a WKAH rat (107). KEG-1, a transplantable rat glioblastoma cell line established from the tumor induced by 1-ethyl-1-nitrosourea in a WKAH rat, was used as an unrelated tumor control (108). K562, a NK cell sensitive human leukemia cell line, was used as a control for the cytotoxicity assay.

Purification of rat DCs was done, as described (109). Briefly, spleen cells of WKAH rats were prepared by incubating minced spleens with collagenase and in RPMI 1640, containing 10% FCS. The spleen cell suspension was cultured overnight on plastic dishes at the concentration of $1x10^8$ cells/dish in medium with $5x10^{-5}$ M 2-mercaptoethnol. After incubation for 24 h, non-adherent cells were collected and placed on the 14.5% Nycodenz gradient. After centrifugation, cells in interphase were collected. Flow cytometrically, collected cells were composed of dendritic cells (70–80%), macrophages (20–30%) and B cells (<5%). To eliminate macrophages and B cells, cells were re-suspended in Hanks' balanced salt solution containing 3% BSA then incubated in a plastic dish for 60 min at 37°C. Non-adherent cells in which the viability exceeded 95% were used as freshly isolated DCs.

For fusion of DCs and KDH-8 cells, polyethylene glycol (PEG) fusion was used. DCs and KDH-8 cells were mixed at a 2:1 ratio and fused by addition of a 50% solution of PEG1500. After washing 3 times with serum free medium, the cells were cultured in medium with 10% FCS for 7 days.

Surface phenotypes of DCs, FCs and KDH-8 were analyzed, using a flow cytometer (Suppl. Fig. 1A). DCs were positive for MHC class I and class II, CD80, CD86 and DC antigen. KDH-8 cells were positive for MHC class I, but negative for class II, CD80, CD86 and DC antigen. After a 7 day culture of fusion cells (the majority of free DCs died under conditions of our culture) and immunomagnetic

depletion of KDH-8, the phenotype of FCs was examined. The FC fraction did not contain morphologically aggregated cells. Although FCs showed the same staining pattern seen in DCs, the expression levels of these surface molecules were significantly decreased, which suggested that most non-fused DCs did not remain in this FC fraction. The fusion between KDH-8 and DCs was also confirmed using a fluorescence microscope (Suppl. Fig. 1B). We used PKH-26-labeled KDH-8 cells in which there was diffuse red staining of the cell membrane. After fusion of PKH-26-labeled KDH-8 cells and DCs, FCs were immunostained with a FITC-conjugated mAb against MHC class II as a cell surface marker of DCs. Many cells of FCs were clearly stained with PKH-26 (red) and with FITC (green).

3) Suppression of tumor growth by FC vaccination *in vivo*

To determine if FCs would induce anti-tumor activity, WKAH rats pre-treated with DC, FCs, or KDH-8 were challenged with KDH-8 cells. All rats pre-treated with either DC or KDH-8 showed no resistance against tumor growth and the transplanted KDH-8 grew in a manner similar to findings in untreated hosts. By contrast, in rats pre-treated with FCs there was a significant delay in tumor development and a reduced tumor incidence. Eighteen of 26 rats were free of tumor at 80 days after injection of KDH-8 (Fig. 47). The resistance to KDH8 was also evident to re-challenged KDH-8 with tumor specificity, since no effect was seen regarding KEG-1 tumor growth (Table 5). Histopathological and immunohistochemical examinations at the tumor injection site in rats given FC vaccine showed numerous lymphocyte infiltrations from the peri-tumor area into the tumor and

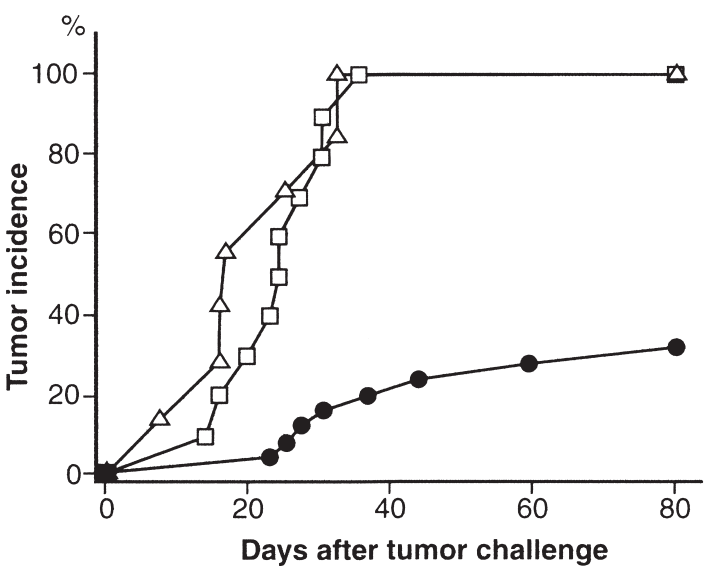

Fig. 47 Suppression of tumor development by FC vaccination. WKAH rats were immunized twice with DCs (△), KDH-8 (□) or FCs (●) then were challenged with KDH-8 at day 4 after the second immunization.

Table 5 Specificity of tumor suppression of rats with acquired resistance to KDH-8 development by FC vaccination.

Tumor cell re-challenged	Rats with tumors/Rats given tumor challenge	
	Rats acquired resistance to KDH-8	Virgin rats
KDH-8	2/8	8/8
KEG-1	3/3	3/3

most of the infiltrating lymphocytes were positively-stained with anti-CD8 mAb (Suppl. Fig. 2A). In contrast, infiltrations of $CD8^+$ lymphocytes were few in tumor biopsies from control rats. Moreover, a considerable number of dead tumor cells was found in many areas of tumor from the FCs-vaccinated rats. Staining with anti-ssDNA mAb revealed that most of the dead cells found among the tumor cells were apoptotic (Suppl. Fig. 2B). In control rats, only a few apoptotic cells were detected. Our findings indicate that FCs vaccination induces $CD8^+$ lymphocyte infiltration into the tumor and rejection of the tumor through the tumor apoptosis induced by CTL activity.

4) Induction of KDH-8-specific CTLs by FC vaccination

To determine if T cells from rats given FC vaccine are responsible for the specific anti-tumor response, splenic T cells from the FCs-vaccinated rats after KDH-8 rejection were re-stimulated by FCs *in vitro* then assayed lytic activity against target cells. The splenic T cells, as effector cells, specifically killed KDH-8 in an effector cell number dependent manner (Fig. 48A and B). No lytic effect was evident when splenic T cells from control rats pre-treated with PBS served as effectors (Fig. 48A), or when the syngeneic glioblastoma line KEG-1 or NK-sensitive K562 cells served as targets (Fig. 48B).

Next, we asked if the tumor rejection induced by FCs vaccination was mediated by $CD4^+$ or $CD8^+$ T cells. In case of pre-treatment of effector cells with anti-CD8 mAb, the lytic activity against KDH-8 was significantly reduced (about 90% inhibition), but anti-CD4 mAb treatment was reduced by only about 40% (Fig. 49). The FCs vaccination induced anti-tumor cellular responses mostly depended on $CD8^+$ T cells-mediated tumor-specific lysis. In addition, pre-incubation of the targets with anti-MHC class I mAb, in general, abrogated tumor lysis, but anti-MHC class II mAb treatment was not effective regarding anti-tumor responses. Results suggest that tumor-reactive effector cells induced by FC vaccination are $CD8^+$ T cells with cytotoxic activity restricted to MHC class I.

5) Humoral response against KDH-8 in rats given FC vaccine and/or KDH-8 challenge

To determine if effective humoral responses can be induced by FC vaccination, sera from FCs-vaccinated rats, FCs-vaccinated and KDH-8-challenged rats, and

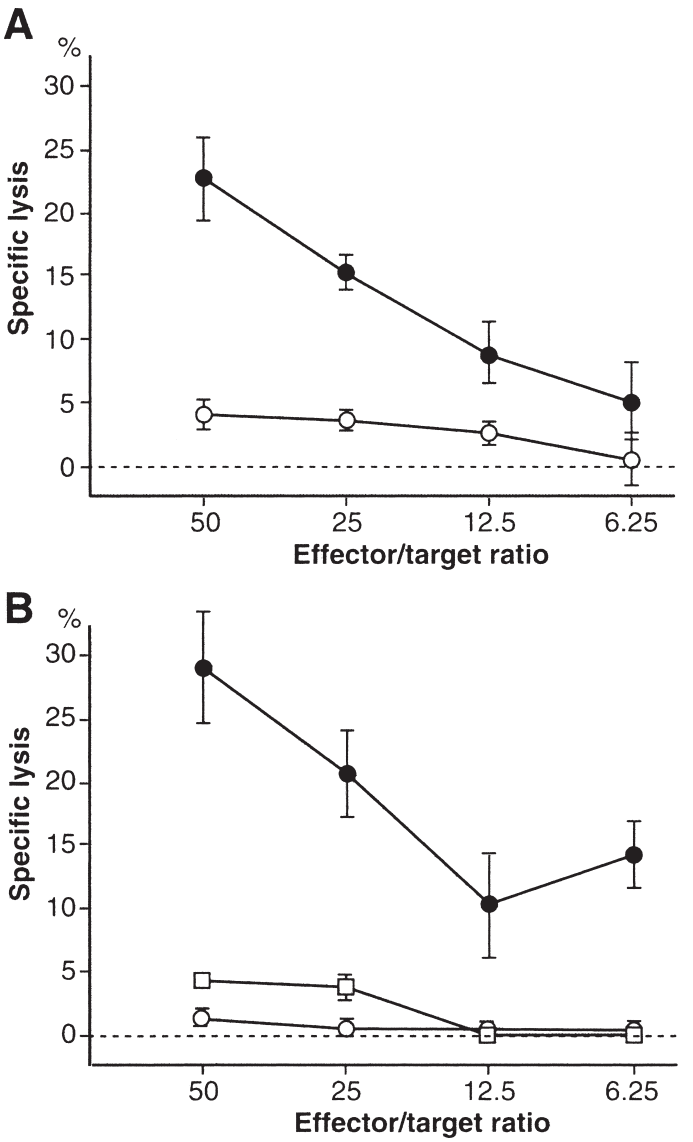

Fig. 48 FC vaccine induces KDH-8-specific CTLs in rats. Splenic T cells from rats immunized twice with FCs (●) or PBS (○) and challenged KDH-8 were isolated at 4 weeks after the KDH-8 challenge and were stimulated with FCs *in vitro*. Then T cells as effector cells were assessed for cytotoxicity against ^{51}Cr- labeled KDH-8 as targets (**A**). To determine specificity of the cytotoxicity, ^{51}Cr- labeled KEG-1 (□) and K562 (○) were used as targets (**B**). The KDH-8 (●) is a positive control.

KDH-8-challenged rats were examined for reactivity against KDH-8, using a flow cytometer. No significant reaction to KDH-8 was evident in sera from FCs-vaccinated rats. Sera from KDH-8-challenged rats regardless of FC vaccination and of tumor growth could react against KDH-8 cells. This suggested that KDH-8 challenge is more effective than FC vaccination to induce an anti-KDH-8 humoral

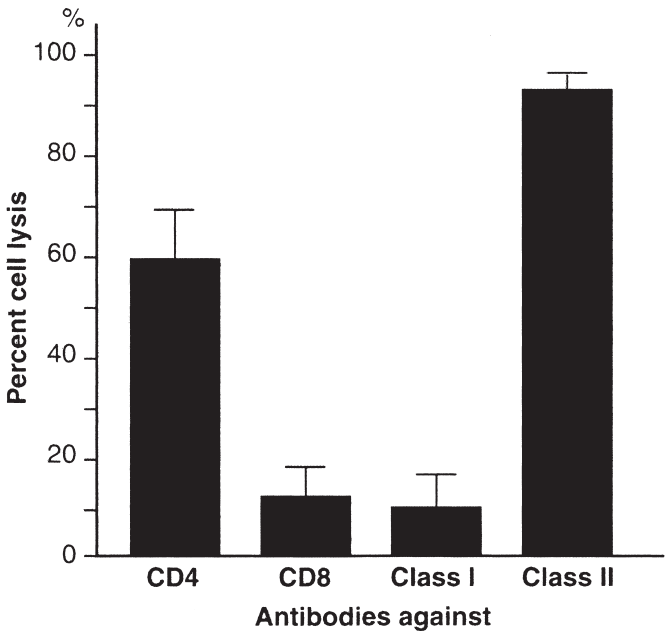

Fig. 49 Majority of the cytotoxic effector cells was CD8 positive with MHC class I restriction.

response and the humoral response was inadequate for KDH-8 rejection *in vivo*.

6) Immunotherapeutic models

To further evaluate CTL activity *in vivo*, *in vitro* amplified effector cells from FCs-vaccinated KDH-8 resistant rats were subcutaneously injected into the right flank of rats, together with KDH-8 cells. The KDH-8 tumor growth was significantly prevented, whereas, the tumor grew normally on the contra-lateral side with injection of KDH-8 alone (Student's t test, $p<0.05$) (Fig. 50). Thus adoptive transfer of effector cells is locally effective in preventing tumor growth when effector cells mixed with tumor cells are injected.

Next, we asked whether local administration of effector cells would prevent tumor recurrence. KDH-8 injected rats underwent surgical resection of a subcutaneous tumor then FCs were injected on the same side at weekly intervals. In rats vaccinated with FCs after surgical resection, 5 of 6 rats showed complete inhibition of the recurrence. In contrast, all rats treated with PBS instead of FCs had a tumor recurrence (Table 6), thereby indicating that local vaccinations with FCs after surgical resection of the tumor can be effective in preventing tumor recurrence.

7) Summary and perspectives

Several reports on immunotherapy using dendritic cells-based vaccine have been published. We investigated findings using FCs generated from rat dendritic cells and a syngeneic hepatic cancer cell line with regard to inducing anti-tumor

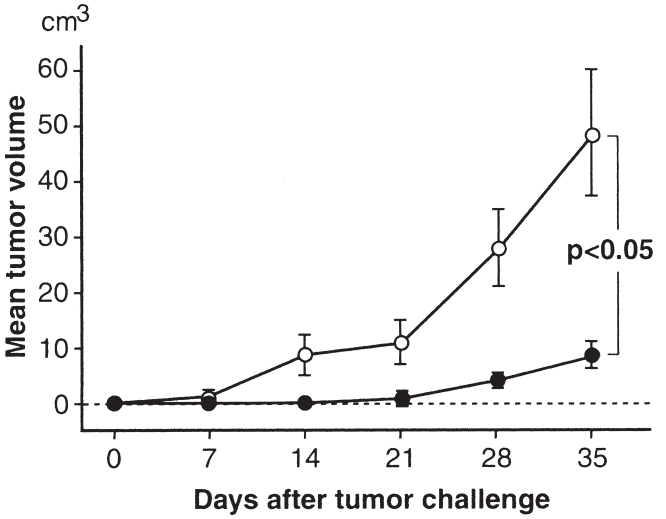

Fig. 50 Prevention of KDH-8 tumor growth in rats given adoptive immunotherapy. Rats given KDH-8 mixed with effector cells (●) prepared from splenic T cells of rats with FC vaccination and KDH-8 challenge or KDH-8 alone (○) at each side of the flank.

Table 6 Protection against tumor recurrence by FC vaccination in tumor-bearing rats after tumor resection.

Treated with	Rats with recurred tumor/Rats examined
FCs	1/6
PBS	6/6

immunity. Vaccination of rats using FCs protected against growth of the subcutaneously implanted tumor *in vivo* and induced infiltration of $CD8^+$ T cells into the tumor. At the site of $CD8^+$ T cell infiltration, there were apoptotic tumor cells. T cells from spleen of FCs-vaccinated rats with protective ability against tumor growth included tumor specific cytotoxic $CD8^+$ T cells restricted to major histocompatibility complex class I. In addition, adaptive transfer of *in vitro* restimulated splenic T cells with FCs was effective in preventing tumor growth and *in vivo* vaccinations of rats with FCs after resection of the subcutaneous implanted tumor inhibited local tumor recurrences. Immunotherapy using FCs appears to be an effective method if used in combination with surgical and/or other anti-cancer therapies.

3. *In vitro* model of suicide gene therapy for alpha-fetoprotein-producing gastric cancer (110)

1) Introduction

Approximately 5% cases of gastric cancer produce alpha-fetoprotein (AFP)

(111). Since the majority of AFP-producing gastric cancer histologically resemble hepatocellular carcinoma, it is termed "hepatoid adenocarcinoma of the stomach" (112). Regardless of recent therapeutic improvements, prognosis remains poor because of frequent vascular invasion and liver metastasis (111, 112). In cancer gene therapy, enzyme-activating prodrug therapy so-called "suicide gene therapy", in which the transgene encodes an enzyme that activates a specific prodrug to create toxic products, is considered to be hopeful (113). Among various combinations of enzyme and prodrug, transfer of the herpes simplex virus thymidine kinase (HSVtk) gene followed by ganciclovir (GCV) administration is a well-characterized protocol. HSVtk converts the protoxic nucleoside analogue, GCV, into a highly toxic phosphorylated form that acts as a chain terminator of DNA synthesis and an inhibitor of DNA polymerase, resulting in induction of death of dividing cells (114–116). The most critical issue in gene therapy is how to selectively target the cells of interest. In this regard, transcriptional targeting can be achieved, using a tissue- or cell-specific promoter to regulate transgene expression (117). Kanai *et al*. (118) reported that adenovirus vectors carrying the constructed AFP enhancer/promoter element induced expression of the HSVtk transgene exclusively in AFP-producing human hepatoma cells, and the following GCV administration efficiently reduced viability of the hepatoma cells *in vitro*. Based on the evidence, we examined the efficacy of suicide gene therapy (the AFP enhancer/promoter-specific transfer of the HSVtk gene followed by GCV administration) against AFP-producing gastric adenocarcinoma cells.

2) AFP secretion from gastric adenocarcinoma cells

To confirm the AFP-production from FU97, an AFP-producing human gastric adenocarcinoma cell line (119), AFP in culture supernatants was quantified, using ELISA kits. Concentrations of AFP in the supernatants of FU97 were 176.2±8.8 ng/ml (mean±standard error (SE) in triplicated wells), whereas those of MKN28, an AFP-nonproducing gastric adenocarcinoma cell line as a negative control, were below the detectable level of the ELISA kit.

3) Comparison of sensitivity to adenovirus vectors

FU97 and MKN28 were infected with Adex1CAlacZ, and X-gal staining was done 24 h later. As a result, 61.33±0.95%, 41.67±2.19%, and 18.33±2.19% of FU97 cells had β-galactosidase activity when the cells were infected with the vector at a multiplicity of infection (MOI) of 100, 10, and 1, respectively (Fig. 51A and Suppl. Fig. 3A). On the other hand, 100±0.00%, 96.67±0.66%, and 34.33±2.59% of MKN28 cells stained blue when the vector was infected at 100, 10, and 1 MOI, respectively (Fig. 51A and Suppl. Fig. 3B). These findings suggest that sensitivity to adenovirus vectors of MKN28 exceeded that of FU97.